COBISS: 1.01

THE CONTRIBUTION OF CONDENSATION-CORROSION IN THE MORPHOLOGICAL EVOLUTION OF CAVES IN SEMI-ARID REGIONS: PRELIMINARY INVESTIGATIONS IN THE KYRENIA RANGE, CYPRUS

PRISPEVEK KONDENZACIJSKE KOROZIJE PRI RAZVOJU JAM V POLSUHIH OBMOČJIH: PREDHODNI REZULTATI V JAMAH KIRENIJSKEGA GOROVJA, CIPER

Didier CAILHOL[1], Philippe AUDRA[2,*], Carole NEHME[3], Fadi Henri NADER[4], Mladen GARAŠIĆ[5], Vasile HERESANU[6], Salih GUCEL[7], Iris CHARALAMBIDOU[8], Lauren SATTERFIELD[9], Hai CHENG[10] & R. Lawrence EDWARDS[11]

Abstract UDC 551.435.84(393.7)

Didier Cailhol, Philippe Audra, Carole Nehme, Fadi Henri Nader, Mladen Garašić, Vasile Heresanu, Salih Gucel, Iris Charalambidou, Lauren Satterfield, Hai Cheng & R. Lawrence Edwards: The contribution of condensation-corrosion in the morphological evolution of caves in semi-arid regions: preliminary investigations in the Kyrenia Range, Cyprus

The condensation-corrosion process occurs when airflow cools at the contact with colder cave walls. Condensed water becomes aggressive for soluble rocks and corrodes the walls. This process is particularly active close to cave entrances in high thermal gradient zones where external air enters caves. Condensation ap-

Izvleček UDK 551.435.84(393.7)

Didier Cailhol, Philippe Audra, Carole Nehme, Fadi Henri Nader, Mladen Garašić, Vasile Heresanu, Salih Gucel, Iris Charalambidou, Lauren Satterfield, Hai Cheng & R. Lawrence Edwards: Prispevek kondenzacijske korozije pri razvoju jam v polsuhih območjih: predhodni rezultati v jamah Kirenijskega gorovja, Ciper

Kondenzacijska korozija se pojavi ob stiku vlažnega zračnega toka s hladnimi jamskimi stenami. Pri tem na jamsko steno iz zraka kondenzira film vode, ki kemično korodira vodotopno kamnino. Proces je najbolj izrazit v bližini jamskih vhodov, kjer ob visokem temperaturnem gradientu zunanji zrak vs-

[1] EDYTEM, University of Savoy - Mont-Blanc - CNRS, Pôle Montagne, 5 bd de la mer Caspienne F-73376 Le Bourget-du-Lac cedex, France, e-mail: didier.cailhol@wanadoo.fr

[2] Polytech'Lab EA 7498, University of Nice Sophia-Antipolis, 930 route des Colles, 06903 Sophia-Antipolis, France, e-mail: audra@unice.fr

[3] UMR 6266 IDEES, University of Rouen - CNRS, 7 rue Thomas Becket, 76781 Mont-Saint-Aignan cedex, France, e-mail: carole.nehme@univ-rouen.fr

[4] Union Internationale de Spéléologie, IFP Energies nouvelles, 1 & 4 avenue de Bois-Préau, 92852 Rueil-Malmaison cedex, France, e-mail: fadi.nader@gmail.com

[5] Croatian Academy of Sciences and Arts, University of Zagreb, Trg Nikole Šubića Zrinskog 11, 10000, Zagreb, Croatia, e-mail: mgarasic@grad.hr, mladen.garasic@zg.t-com.hr

[6] CINaM, CNRS - Aix-Marseille University, Campus de Luminy, case 913, 13288 Marseille cedex 9, France, e-mail: heresanu@cinam.univ-mrs.fr

[7] Environmental Research Center, Near East University, Nicosia, Cyprus, e-mail: sgucel@hotmail.com

[8] Department of Life and Health Sciences, School of Sciences and Engineering, University of Nicosia, Nicosia, Cyprus, e-mail: charalambidou.i@unic.ac.cym

[9] School of Environmental and Forest Sciences, Box 352100, University of Washington, Seattle, Washington 98195, USA, e-mail: lauren.c.satterfield@gmail.com

[10] Xi'an Jiaotong University, Qujiang Campus, No.28 Xianning West Road, Xi'an, Shaanxi, 710049, P.R. China, e-mail: cheng021@xjtu.edu.cn

[11] University of Minnesota, Department of Earth Sciences, Newton Horace Winchell School of Earth Sciences, 3 Morrill Hall 100 Church St. S.E. Minneapolis MN 55455, USA, e-mail: edwar001@umn.edu

* Corresponding author

Received/Prejeto: 09.09.2018

DOI: https://doi.org/10.3986/ac.v48i1.6782

pears to be important where bat colonies are also present. Bat metabolism and guano decomposition release heat, vapour, and acids. Hence, bat colonies contribute to the increase of condensation-corrosion, especially by providing permanent moisture and chemical aggressiveness. Corrosive air convections produce rounded morphologies, such as ceiling channels, cupolas, and corroded older flowstones. This process has been overlooked in previous research, since related morphologies were often confused with those produced by early phreatic flow. Kyrenia Range in Cyprus has a semi-arid climate. All the studied caves developed along open-fractures. They are located both in recrystallized carbonates (limestone and dolostone, such as Smoky and Pigeons Caves), or in gypsum (First Day and Angry Bat Caves). We also studied a maze cave that acted as a spring in gypsum that initially developed under phreatic conditions, followed by an epiphreatic phase that allowed the development of notches (Fig Tree Cave, also named İncirli Show Cave). Due to the semi-arid climate, external air is very dry in summer, thus condensation seems to occur mainly in winter, when cave atmosphere instability allows large air exchanges between caves and surface atmosphere. In summer, evaporation prevails, allowing the development of popcorn lines in carbonate caves and massive gypsum crusts, stalagmites, and sidewalk rims in gypsum caves. However, the presence of a bat colony in a semi-confined chamber in Smoky Cave is probably the origin of the permanent moisture, also during the dry season, leading to a strong development of condensation-corrosion features such as ceiling cupolas, and possibly to the permanent activity of flowstones. In addition, we detected high concentrations of sulphur dioxide (SO_2) and radon (Rn) in Fig Tree Cave, possibly related to the activity of the neighbouring overthrust. Based on the five studied caves in the Kyrenia Range and surroundings, the open-fracture caves in carbonates and gypsum have not undergone the typical initial phreatic stage, but have formed in a short time during Pleistocene as a result of the fast uplift of the range and were later reshaped by condensation-corrosion morphologies. Some gypsum caves may have formed entirely by this latter process, after initial minor fracture development. Cyprus is an outstanding area for studying the condensation-corrosion in caves, since a phreatic origin can be ruled out for most of the rounded morphologies.
Key words: East-Mediterranean, condensation-corrosion, guano, Kyrenia Range-Cyprus, open-fracture-caves, fast tectonic uplift, gypsum, cave microclimatology, Pleistocene.

topa v jamo. Kondenzacijo in kondenzacijsko korozijo lahko pomembno povečajo kolonije netopirjev. Metabolizem netopirjev in razpadanje gvana sproščata toploto, vlago in kisline. Kondenzacijska korozija iz konvekcijskih tokov vlažnega zraka ustvarja zaobljene skalne oblike, kot so kupole, stropni kanali in korodirana siga. Kirenijsko gorovje na Cipru ima polsuho podnebje. Večina jam v tej raziskavi so odprte razpoke v prekristaljenem karbonatu (apnenec in dolomit) ali v sadri. Poleg teh obravnavamo tudi blodnjake v sadri, ki so se oblikovali v freatični coni in so v preteklosti delovali kot izviri. V njih najdemo stenske zajede, ki so nastale v epifreatični fazi. Ker je zrak poleti zelo suh, je kondenzacija omejena na zimski čas, ko se intenzivno izmenjuje zrak med jamsko in zunanjo atmosfero. Poleti prevladuje izhlapevanje, kar omogoča razvoj cvetačastih oblik v karbonatnih jamah ter sadrinih skorij, stalagmitov in stranskih obrob v jamah v sadri. Kolonija netopirjev v eni od polzaprtih dvoran v jami Smoky Cave verjetno vzdržuje visoko vlago tudi poleti. Posledica so močno izražene oblike kondenzacijske korozije (kupole) in stalna aktivna rast sige. V eni od jam smo izmerili visoko vsebnost SO_2 in radona, ki je verjetno povezana z aktivno narivno tektoniko. Pet obravnavanih jam je tektonskega izvora in so verjetno nastale v kratkem obdobju hitrega dvigovanja v pleistocenu ter bile kasneje preoblikovane s kondenzacijsko korozijo. Nekatere jame v sadri so nastale skoraj izključno s kondenzacijsko korozijo, ki je preoblikovala prvotne majhne razpoke. Ciper je izjemno območje za podobne študije, saj lahko zaradi odsotnosti freatične faze večino zaobljenih jamskih oblik pripišemo kondenzacijski koroziji.
Ključne besede: Vzhodno Sredozemlje, kondenzacijska korozija, gvano, Kirenijsko gorovje, jame v odprtih razpokah, hitri tektonski dvig, sadra, jamska mikroklima, pleistocen.

INTRODUCTION

The condensation-corrosion process corresponds to the dissolution of cave walls by condensation water brought by external airflow crossing caves and cooling on colder walls. This widespread process is particularly efficient in relict caves, close to entrances where the thermal gradient is high, in alpine caves where airflow is substantial, in the upper levels of cave or close to the ceiling where air is warmer (Badino 1995, 2010), or in hypogene caves when corrosion is enhanced by the presence of acids. It is far more active in summer when cooling of surface air entering caves can produce significant amounts of condensation; in contrast, condensation is very limited in winter, except in alpine caves when air rising through vertical caves cools and produces condensation in upper entrances, at the contact of the rock cooled by the ambient winter temperature (Klimchouk *et al.* 1996; Dublyansky & Dublyansky 2000). Several studies have shown the relative importance of condensation water volume: in the Crimea region, it represents 3.5% of the total spring discharge and 4.5 L/s/km^2 in summer (Dublyansky & Dublyansky 2000), 0.7 L/s in the Sorbas semi-arid region, Spain (Sanna *et al.* 2015), 0.15 L/s in Spipola Cave, Italy

(Cigna & Forti 1986), and 0.1 L/s in the Dent de Crolles system, France (Lismonde 2002).

Condensation acquires its aggressiveness from CO_2 in the cave air and becomes corrosive for the limestone walls (Dreybrodt *et al.* 2005). Wall retreats have been calculated, theoretically (Dreybrodt *et al.* 2005), from field climate records (Dublyansky & Dublyansky 2000), from corrosion measures on limestone tablets (after P.M. Avramides in James 2013; Tarhule-Lips & Ford 1998a), and from uranium-thorium (U/Th) dating on corroded speleothems (Auler & Smart 2004). These studies suggest a wall retreat range from 0.3 to 30 mm/ka. In Sorbas gypsum caves, wall retreat has been estimated to be 22–33 mm/ka (Klimchouk *et al.* 1996; Gázquez *et al.* 2015; Sanna *et al.* 2015). In extreme environments, such as in hypogene caves with high concentration of acidic gas and high thermal gradient, the intensity of condensation-corrosion and of the wall retreat is 1 to 2 orders of magnitude larger (Lismonde 2003; Dublyansky & Dublyansky 2000 and references therein). Special attention has recently been given on caves occupied by large bat colonies. The metabolism of bats and the mineralization of guano produce CO_2, vapour, and heat. Together, they contribute to the increase of the condensation-corrosion process with a wall retreat reaching up to 34 mm/ka. In some peculiar cases, bat-related condensation-corrosion appears to be the main process of cave enlargement (Lundberg & McFarlane 2012, 2015). The morphologies related to this process are cupolas, bell holes, flutes, megascallops, pendants, karrens, ceiling channels, corroded or weathered walls, boxwork, and potholes (Cigna & Forti 1986; Jameson 1991; Tarhule-Lips & Ford 1998a, b; Auler & Smart 2004; Lundberg & McFarlane 2009; Miller 2014; Fabbri *et al.* 2017; Frumkin *et al.* 2018; Audra *et al.* 2016 and references therein).

The condensation-corrosion process, enhanced by airflow convections, shapes rounded features (such as ceiling channels, niches, convection cupolas, and megascallops), which are almost similar to the phreatic morphologies in “classical” cave passages. The superimposition of features associated with both processes is frequent and occurs successively, first by phreatic and then aerial processes. Therefore, measuring the condensation-corrosion process separately is difficult in caves initially formed in a phreatic context, thus making the quantification of this particular process challenging. Therefore, the condensation-corrosion process has been under-estimated as a significant morphogenic process, compared to phreatic flow, which is indeed widespread.

The Kyrenia Range is located along the northern coast of the island of Cyprus, paralleling the northern shore (Fig. 1). The Kyrenia Range, a 160 km long, narrow mountain range with a maximum elevation reaching 1000 m a.s.l., was subject to a rapid uplift and aerial exposure only since the Upper Pliocene. Most of the caves found in the range are therefore of tectonic origin, not dissolutional karstic, comprising original rounded voids that were never under phreatic conditions. Thus, this Mediterranean region and its related caves provide an excellent focus for the investigation of “rounded” features linked to condensation-corrosion by airflow convections.

In this paper, we analyse the condensation-corrosion features of five caves in carbonate and gypsum rocks located in the Kyrenia Range, Cyprus, in order to: i) define the morphological features as an expression of cave genesis; ii) characterize the morpho-tectonic evolution; iii) assess the role of condensation-corrosion as a major late stage process in semi-arid climate; iv) highlight the role of bat colonies and guano deposits.

THE KYRENIA RANGE (GEOLOGY, GEOMORPHOLOGY, CLIMATE, VEGETATION)

Cyprus is located in the Levantine Basin, in the Eastern Mediterranean region (35°N; 33°E). It is the third largest island in the Mediterranean Sea, with a surface of 9250 km^2 (Fig. 1). Three major physiographic units characterize the island. The Troodos Mountain is the main mountain range on the island, reaching 1951 m a.s.l. (Mt. Olympus). The narrow belt (6 km wide and 160 km long) of the Kyrenia Range along the northern coastline rises to 1023 m a.s.l. to the West (Kronos Peak), and lowers eastward until the tip of the Karpas Peninsula. Both ranges are separated by the Mesaoria Plain, which has an average altitude of 100 m a.s.l. (max. 325 m a.s.l.), and where Nicosia, the capital city, is located.

Cyprus is at the junction of the African Plate to the South, the Anatolian microplate to the North, and the Arabic Plate to the East (Fig. 2a). The Kyrenia Range is mainly composed of Triassic to Cretaceous limestones and dolomitic limestones, recrystallized in marbles (Constantinou 1995). To the south of the Kyrenia range, the Mesaoria Plain is filled with mainly marine sediments dated from the Paleogene to Quaternary. The present-day island structure expresses dextral movements associated with the northward motion of the African and Arabian

Fig. 1: Kyrenia Range is a narrow mountain range along the northern coast of Cyprus. It is made up of Carboniferous to Miocene rocks, mainly recrystallized limestones and dolostones. Troodos Mountain is made up of ophiolites surrounded by Cretaceous to Middle Miocene rocks. In-between, the Mesaoria Plain, together with the coast, are built by a layer of Miocene to recent sediments. The studied caves in Kyrenia Range are indicated by red dots.

plates that were at the origin of the westward escape of the Anatolian microplate, with permanent and significant seismic activity (up to 6.5 magnitude). The orogenesis of the Kyrenia Range occurred in the Late Miocene / Early Pleistocene, when the southern margin of the Anatolian microplate folded and overthrusted onto the Troodos massif with a left-lateral and transpressional regime. A regional uplift intensified during the Early Pleistocene, controlled by under-thrusting of continental crust from the south (Constantinou 1995; Palamakumbura & Robertson 2016; Harrison *et al.* 2013). The carbonate Trypa Formation ranging from the Triassic in the north to the Cretaceous in the south settled as subvertical slabs and narrow folds that preserve more recent chalky layers from the Lapithos Formation, from Cretaceous to Eocene (Fig. 2b). The center of the Kyrenia Range landscape is marked by the Kyrenia Crest with olistostrome of permo-carboniferous Kantara limestones. The southern edge is overthrusted over the Cenozoic Kythrea Formation of the Mesaoria Plain, along the active frontal transpressive thrust of the Kyrenia Range (Fig. 2c). The northern edge of the range comprises limestone bars covered with sediments, from Cenozoic to recent formations (McCay & Robertson 2013).

From the geomorphological point of view, the highest part of the range displays sharp blades corresponding to subvertical carbonate slabs. They are locally truncated by subhorizontal ledges, elongated according to the range axis (Fig. 3). The range is delimited either by E-W fault escarpments, or by successive pediment slopes that connect to the Mesaoria Plain in the south and extend below the current sea level in the north. Along the northern slope of the pediments, several levels of terraces, located between 1000 m a.s.l. to the present sea level, display some ledges. Some high terraces comprise megabreccia and colluvium deposits, while others are composed of marine deposits. The successive terraces record previous sea levels and allow the estimation of the uplift rate since the Upper Pliocene / Lower Pleistocene to the Quaternary period. According to Harrison *et al.* (2013) and Palamakumbura *et al.* (2016), uplift rates during the Quaternary were fast at the beginning, then slower. Surficial karst features are limited to few morphologies: i) recent rain karren; ii) round karren exhumed by *terra rossa* erosion due to previous deforestation and forest fires on the upper terraces (Fig. 4); iii) small uvalas and intramountain flat basins developed from the soft chalky Lapithos layers and covered with *terra rossa*; iv) ancient travertine plateaus such as the site along the main road above Kyrenia city (Necdet 2003).

The climate of Cyprus is semi-arid with mean monthly temperatures ranging from 21 °C along the coast to 15 °C on top of the Kyrenia Range. Temperature maxima can reach 35–45 °C in the Mesaoria Plain. Rainfall is mainly concentrated in the winter season (October to March), with annual minima of 342 mm in the sheltered Mesaoria Plain and up to 550 mm annually on the Kyrenia Range, which acts as a barrier for the northern marine winds (Fig. 5) . The evapotranspiration reaches 90% with a small specific recharge amount of 4 L/s.km^2) for the wettest reliefs. In a tectonic context of extreme fracturation, the infiltration occurs over 85 km^2 along a narrow carbonate range and eventually reaches very small overflow springs located at the foot of the range near archeological and historical sites: Kythrea, Bellapais, Lapithos, Krini, and Karavas (Unit of Environmental Studies 2018).

The vegetation cover in northern Cyprus is typical of the semi-arid climatic East-Mediterranean region. It is mainly composed of herbaceous and garrigue forests on the lower slopes. The summits of the northern slopes are covered with pines and cypress forest and degraded Mediterranean scrub after repeated fires.

The Kyrenia carbonates seem to be poorly karstified, according to the dry climatic conditions, the limited outcrops along the crest, the diffusion of seepage across nu-

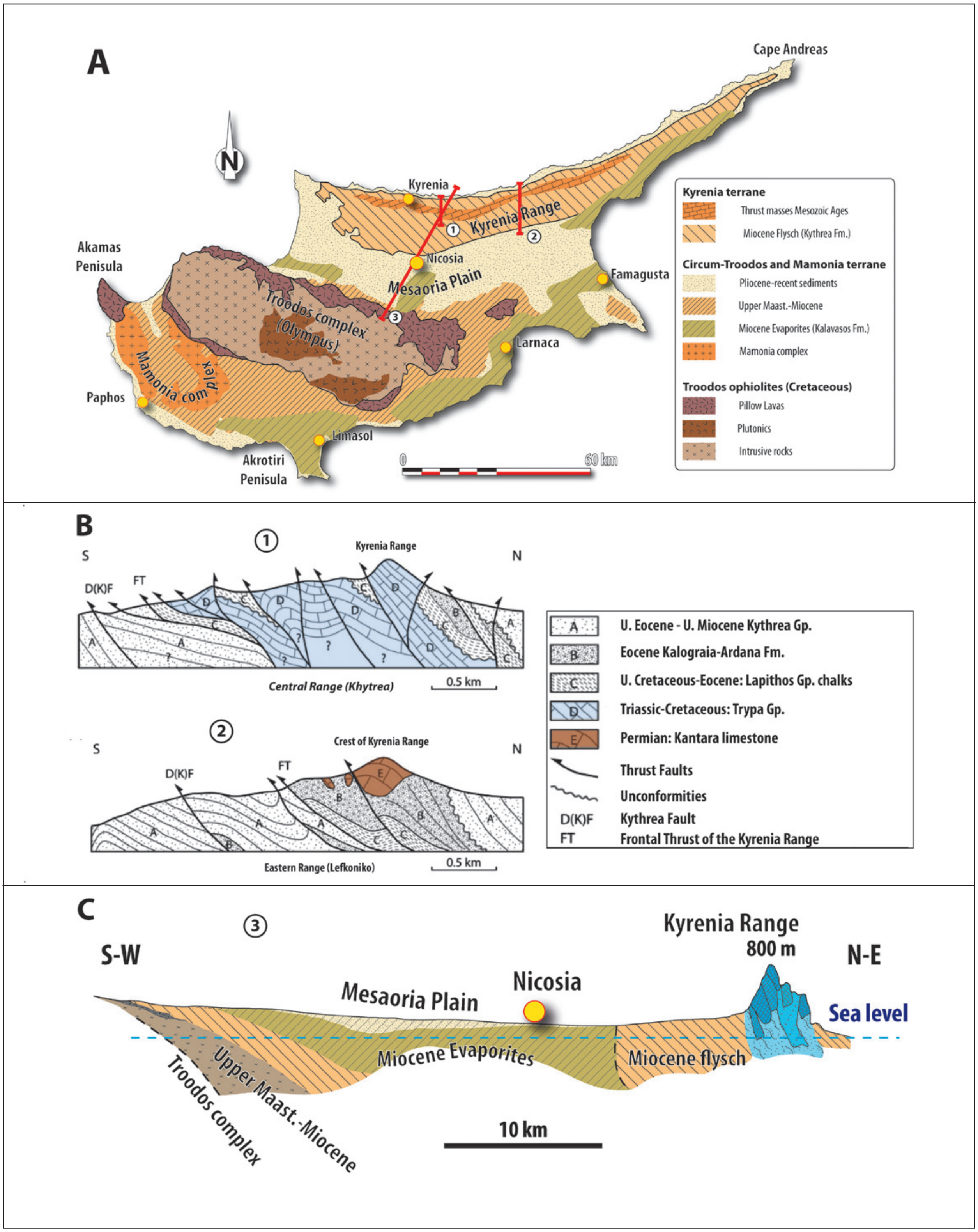

Fig. 2: Geology of Cyprus. A) Kyrenia Range is part of the Anatolian microplate, thrust southward onto the Troodos ophiolites. Kyrenia Crest is made up of subvertical Mesozoic carbonates, and in the eastern part of a Permian limestone olistostrome. B) and C) Geological profiles over sections, indicated on the map A). Data on A) and C) obtained from Cleintuar et al. (1977), and B) from McCay & Robertson (2013).

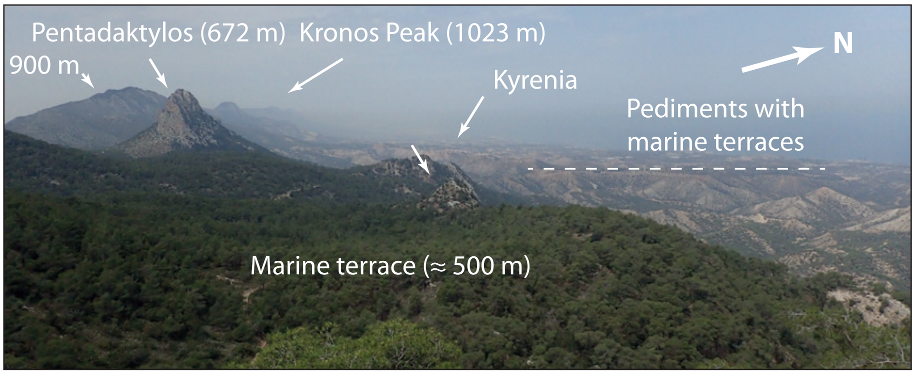

Fig. 3: View of the Kyrenia Range toward the west, with north coast and Kyrenia city to the right (Photo: D. Cailhol).

Fig. 4: Round karren exhumed after soil erosion on a plateau feature located above St. Magar monastery (Photo: P. Audra).

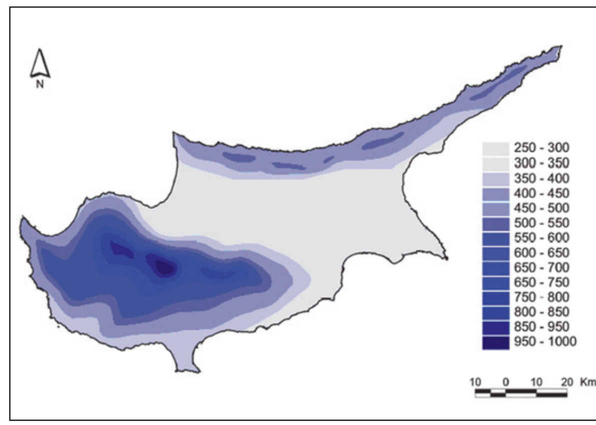

Fig. 5: Distribution of annual rainfall (in mm) in Cyprus (Department of Meteorology 2018).

merous fractures, and the partitioning of catchments by faults. On the surface it is limited to recent rainfall karrens and no typical solution caves were observed. Only some calcite hydrothermal veins associated with early tectonic phases prior to emersion have been identified in marble brecciated zones above St. Magar monastery.

STUDIED CAVES AND METHODOLOGY

Almost 200 caves are recorded in Cyprus (Gucel 2018) and can be grouped in three different types: i) fracture-caves mainly located in massive carbonates (Kyrenia); ii) gypsum caves located in the Messinian gypsum of Mesaoria basin; iii) marine caves located in recent calcarenites (Fig. 1). The caves are of moderate extension. Currently, Fig Tree Cave ("İncirli Show Cave") is the longest cave in Cyprus (365 m), while the deepest is Pentadakty-

Tab. 1: Caves that were surveyed.

Name of Cave	District	Coordinates	Altitude (m a.s.l.)	Vertical range (m)	Length (m)
Smoky Cave	Kyrenia	35.311947°N 33.592556°E	790	35	93
Pigeons Cave	Famagusta	35.421372°N 33.958214°E	477	30	C70
First Day Cave	Famagusta	35.322167°N 33.793594°E	265	≈5	79
Angry Bat Cave	Famagusta	35.322678°N 33.797353°E	310	17	110
Fig Tree Cave	Famagusta	35.324947°N 33.769764°E	245	25	365

los Cave (-200 m). Caves generally host bat colonies and pigeons that produce thick guano deposits. We studied five caves from type i) and ii) (Tab. 1).

THE CAVES IN MASSIVE PERMO-CRETACEOUS CARBONATES (TYPE [I])

Most of the caves are orientated N30°E and correspond to large open-fractures combined with the E-W transpressive faults. These N30°E fractures are strike-slip faults that end up as pull-apart openings (Harrison *et al.* 2008). Some of these openings became fracture-caves, with an initial preserved morphology: mechanical fracture-guided passages, rough and planar walls and ceilings, no trace of any concentrated water flow or fluvial sediments. Due to recent tectonic activity and gravity release movements, subsequent breakdown blocks are covering the bottom-end of shafts. Few of the recent developed fractures derive from decompression near cliffs, even if caves are very close to steep slopes or cliffs because of the thinness of the range. Most fracture-caves are several meters wide and generally limited to dozens of meters deep. Despite their tectonic origin, fracture-caves display a fairly good stability.

Smoky Cave

Mr. Meraklı indicated Smoky Cave entrance. It opens at the edge of the Kyrenia Crest (Fig. 1). The cave developed along an inclined opened fault, oriented N30°E, in recrystallized Triassic dolostone with subvertical dip. It is composed of two successive shafts, 16 and 10 m deep, respectively (Fig. 6). At the bottom of each shaft, the cave opening extends laterally along the fault, as large passages about 30 m long and 5 m wide. The cave is well decorated. In the first shaft, numerous curtains of speleothems have developed along the overhanging wall and were dry on the day of the visit (May 2018). Most of the stalagmites appeared inactive, corroded on the surface, and covered with brown crusts (Fig. 13A). On the contrary, in the Bottom Chamber, calcite formations are abundant, such as stalactites, stalagmites, and flowstones. They were wet and appeared active (Fig. 15A). A colony of bats (*Pipistrellus pipistrellus*) of several hundreds of individuals was present in a cupola of the deeper chamber. Guano is present as extended old dusty deposits at the bottom of the first shaft, and as fresh accumulations in the First Chamber and Bottom Chamber. A strong convective airflow exists at the entrance, with decreasing intensity at depth. The outflowing part of the loop made up of warm and wet air produces a plume of vapour when outside air is cooler (at night and in winter), hence its name "Smoky Cave".

Pigeons Cave

Pigeons Cave opens on top of the crest of one of the easternmost reliefs of the Kyrenia range, 3.5 km east of Kantara castle (Fig. 7). The cave develops along an inclined opened fault, orientated N30°E, in recrystallized Permo-Carboniferous Kantara limestone cropping out as a blade limited on both sides by E-W transpressive faults. It is composed of two shafts of about 15 m each. At the bottom, the fracture extends on both sides as a passage of 1 to 2 m wide. Airflow is present in the northern side of the passage, showing a connection with the neighbouring surface.

CAVES IN THE MESSINIAN GYPSUM (TYPE [II])

Three gypsum caves have been studied in the area around Platania village, in the Famagusta district. The Messinian gypsum of the Kalavasos Formation corresponds to evaporite deposited in a marginal basin during the first

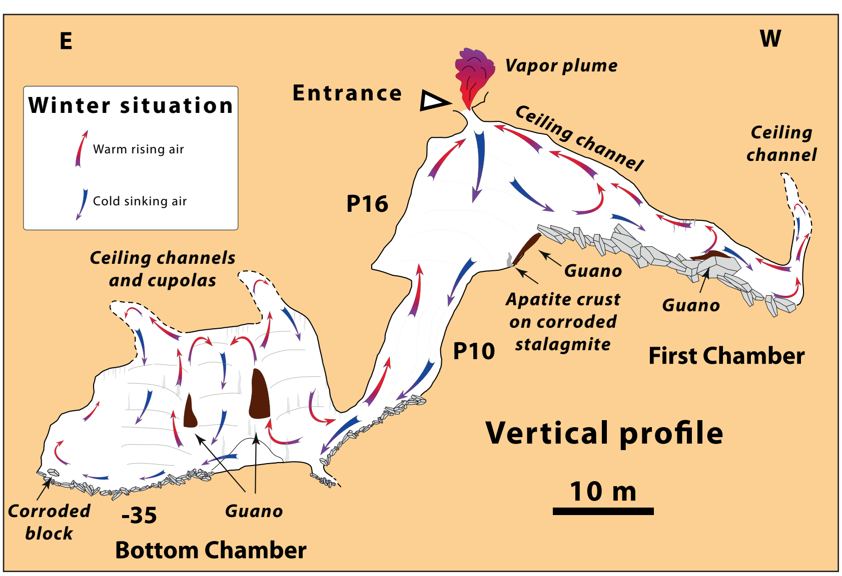

Fig. 6: Vertical profile of Smoky Cave (survey after Spéléo-club du Liban 2018, in collaboration with the Caves of Kyrenia Mountains Project). Micro-climatic winter situation, with airflow observed or inferred from the morphology. Sinking cold air (below 5 °C or sometimes 0 °C) produces a convective loop. Wet (100% RH) and warm (15.2 °C) air at depth is pushed up and gradually cools while rising, producing condensation on the cold ceiling. It carves a condensation-corrosion ceiling channel in massive rock. Subsequent runoff flowing along the overhanging wall gradually saturates, warms, and forms curtains. Finally, the outflowing warm-wet air creates a plume of vapour while mixing with outer cold air, hence its name "Smoky Cave".

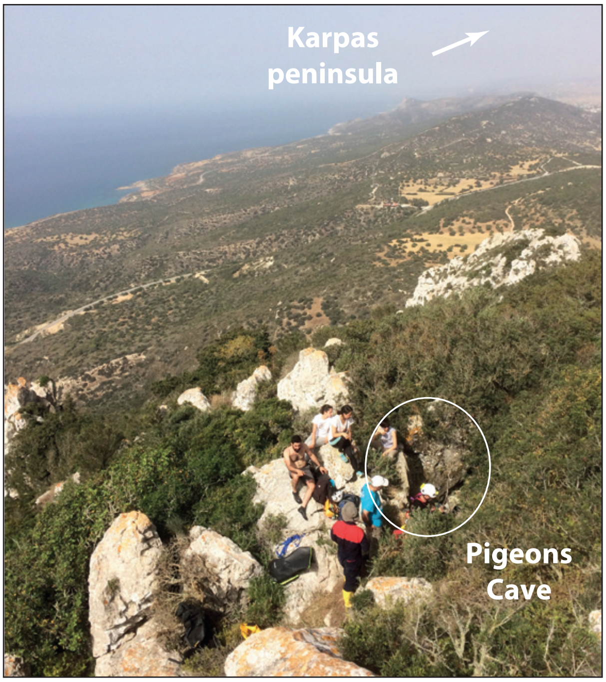

Fig. 7: Pigeons Cave (at the feet of the group, in the circle), opens in Kantara permo-carboniferous limestones bounded by E-W transpressive faults. View to the east, toward Karpas peninsula (Photo: P. Audra).

stage of the Messinian Salinity Crisis (MSC) (Fig. 2A). These deposits were exposed to erosion and karstification during the second major phase of the MSC, before being flooded and buried after the Pliocene transgression (Mocochain *et al.* 2012).

The gypsum strata, about 50 m thick, are located on the top of the Middle Miocene Kythrea Formation, which is composed of marls and sandstone flyschs (Harrison *et al.* 2008). The gypsum strata display several facies: the base is made up of an approximately 10 m thick layer of large selenite crystals, which breaks down as big boulders along the south slope. The rest of the strata is mainly made up of saccharoid gypsum. Close to the top of the plateau, a more calcitic-bedded layer, about 1 m thick, disaggregates as large and thin slates. The gypsum strata crops out as a monocline, with a gentle dip (≈15°) to the north. To the north of the area, at the foot of the Kyrenia range, the Kythrea Formation displays a strong dip, implying the probable presence of an important overthrusting (Fig. 2B). The area displays as an inclined plateau limited to the south by a 100 m high cliff above the Mesaoria Plain and cut by small valleys (Fig. 8). Two types of cave are present: i) caves on top of the cliff developing along a decompression fracture (First Day and Angry Bat caves); ii) paleo-spring cave (Fig Tree Cave).

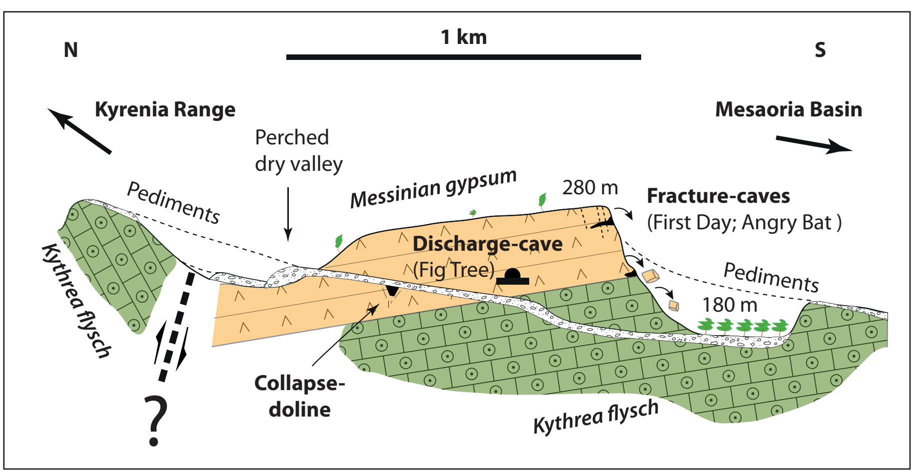

Fig. 8: Simplified sketch of the gypsum monocline cut by a perched dry valley. Fracture-caves open at the top of the crest. Fig Tree Cave opens a few meters above the dry valley.

Fig. 9: Entrance of First Day Cave, at the top of the southern gypsum cliff, looking at the Mesaoria Plain and Famagusta Bay in the distance. The cave develops along decompression fractures parallel to the cliff, which prepare the detachment of blocks. About 50 m below the crest, the gypsum rests on marls and sandstones of the Kythrea Formation (Photo: P. Audra).

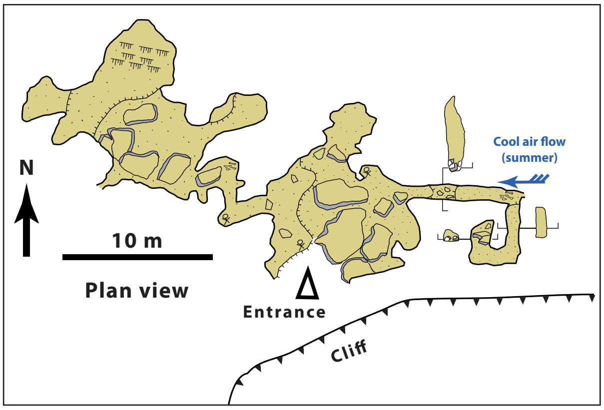

Fig. 10: Topography of First Day Cave (after M. Abercrombie in Chirol & Savoi 2015).

First Day Cave

First Day Cave opens below the top of the cliff as a large entrance (6 m high; 4 m wide), prolonged by a 15 m long gallery (Figs. 9 & 10). At 10 m from the entrance, side passages are located on both sides. To the West, a 15 m long descending low passage harbours lateral rounded niches. To the East, a narrow and 5 m high and 15 m long ascending fracture rises up to a narrow passage plugged by collapsed blocks, close to the plateau surface. Both lateral passages develop along an open-fracture parallel to the cliff. A strong and cool (summer) airflow crosses the cave downward from the East passage to the entrance.

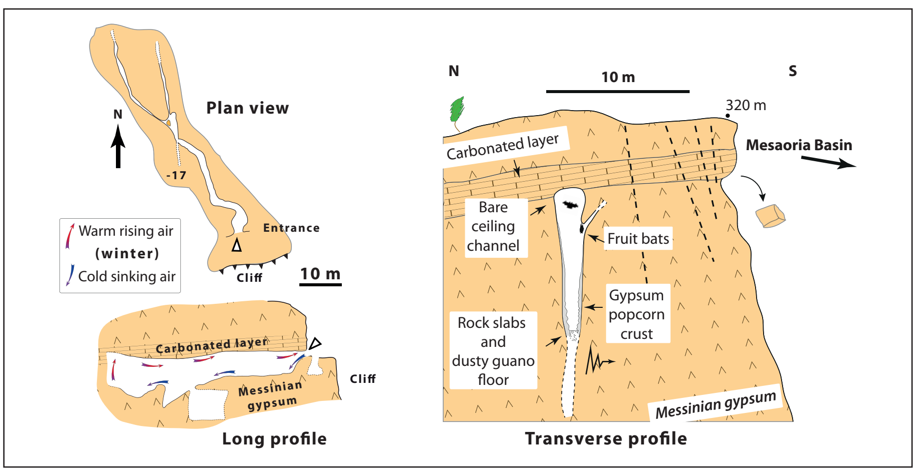

Fig. 11: Topography of Angry Bat Cave (after Chirol et al. 2017), and schematic transverse profile. The cave develops along a decompression fracture that did not affect the carbonated ceiling. Condensation-corrosion occurs in the wet upper part, whereas gypsum crust made by evaporation cover the dry lower part.

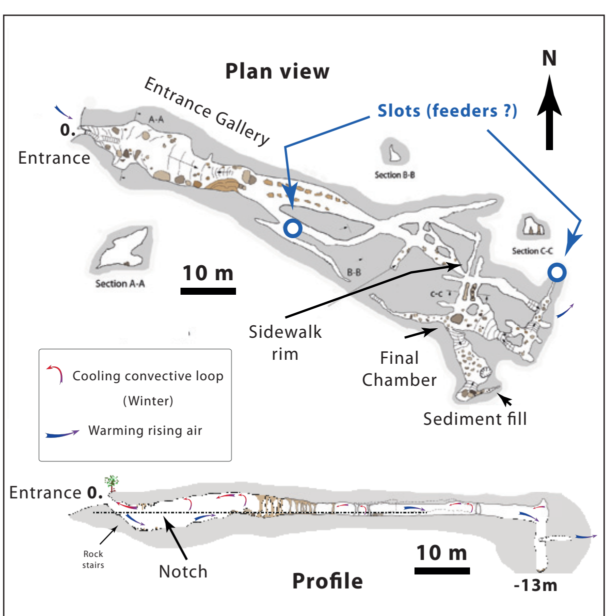

Fig. 12: Fig Tree Cave, plan view and profile (after Chirol & Savoi 2015), with indication of airflow direction in winter, at the origin of condensation-corrosion on the ceiling.

Angry Bat Cave

The entrance of Angry Bat Cave is similar to that of First Day Cave, 350 m to the East. The cave has developed along a decompression fracture, perpendicular to the cliff, as a 10 m high passage, 3 m wide at the entrance and narrowing to 0.5 m, and about 40 m in length (Fig. 11). The ceiling corresponds to the more calcitic-bedded layer that is not affected by the decompression fracture. Pigeons were nesting in the first part and Egyptian fruit bats (*Rousettus aegyptiacus*) observed in the inner part.

Fig Tree Cave

Fig Tree Cave ("İncirli Show Cave") opens about 20 m above the floor of a perched dry valley crossing the gypsum plateau (Fig. 8). The cave displays a maze pattern along fractures, with a 5 m wide and 6 m high main passage at the entrance and smaller fracture-guided passages in the middle part, with a large Final Chamber (Fig. 12). Massive gypsum stalagmites are abundant. Air coming from the overlying plateau is flowing downward (in summer) toward the entrance. Bat guano is present, especially in the end-part, as extended thick (>0.5 m) dry deposits covering the floor.

METHODOLOGY

Some caves were previously mapped and studied by several groups (Jones & Rigby 1962; Jorgenson 1978; Satterfield 2015; Chirol & Savoi 2015, Spéléo-Club du Liban 2018). In addition to previously published data, we used a DistoX2 for additional cave survey combined with photographic documentation of morphological features. Climatic data were recorded using pSENSE RH portable CO_2 meter by Senseair, with an accuracy of ±0.6 °C for temperature, of 3% for RH < 90% and 5% for RH > 90%, and 30 ppm ±5% for CO_2 concentration. Radon concentration was measured in Fig Tree Cave during both the rainy and dry season (March and October 2017, respectively) using Sarad® DOSEman PRO dosimeter, with an accuracy of 150 cpm @ 1000 Bq/m³ (EEC). Guano and sediments mineralogy were identified by XRD at CINaM (CNRS and Aix-Marseille University), XRD patterns were recorded with Panalytical Xpert Pro, θ - θ geometry, Cu radiation (λ=0.15418 nm). ICDD-PDF2 database was used for phase identification. Three speleothems were sampled to constrain the age subsequent to the cave-opening phase. Two stalagmites were retrieved from Smoky Cave growing directly on the calcite flowstone sealing the cave floor. One stalagmite was sampled from Pentadactylos Cave at 50 m deep from the shaft entrance. Stalagmites were sampled from their base and the U-Th dating was conducted in Xi'an Jiaotong University, China (Tab. 4). Activity ratios were determined using a NU Plasma MC-ICP-MS following the procedure of Cheng *et al.* (2013).

RESULTS

SMOKY CAVE

The temperature was 17.7 °C at the bottom of the entrance shaft (May 2018) and 15.2 °C at the bottom of the cave (Dec. 2017 and May 2018), which differ by +1.4 °C and -1.1 °C from the local mean annual temperature (16.3 °C), respectively (Tab. 2). Relative humidity (RH) was 88.6% at the bottom of the first shaft, and 99.9% in the Bottom Chamber (May 2018). The first shaft appeared completely desiccated by entering dry air, whereas some places in the First Chamber ceiling showed discrete dripping originating from reliefs in massive rock with no apparent fissure, thus attributed to condensation. No seepage from surface was visible in May 2018. The Bottom Chamber was entirely wet, and moisture seemed to come entirely from condensation without seepage contribution during early-summer season.

Below the fresh guano deposits, where dripping provided moisture, calcite flowstones were tinted in dark brown, yellow and orange. DRX analysis of the brown crust covering the old corroded stalagmite of the first shaft (Fig. 13) indicated the presence of phosphate (hydroxylapatite), related to the mineralization of the neighbouring guano, associated to detrital components (quartz, illite), to some gypsum, and possibly to magnesian calcite (Fig. 13, Tab. 3). Possible phillipsite was detected; however, such zeolite mineral is unlikely in this environment, unless it is of detrital origin.

Some rounded features morphologies were identi-

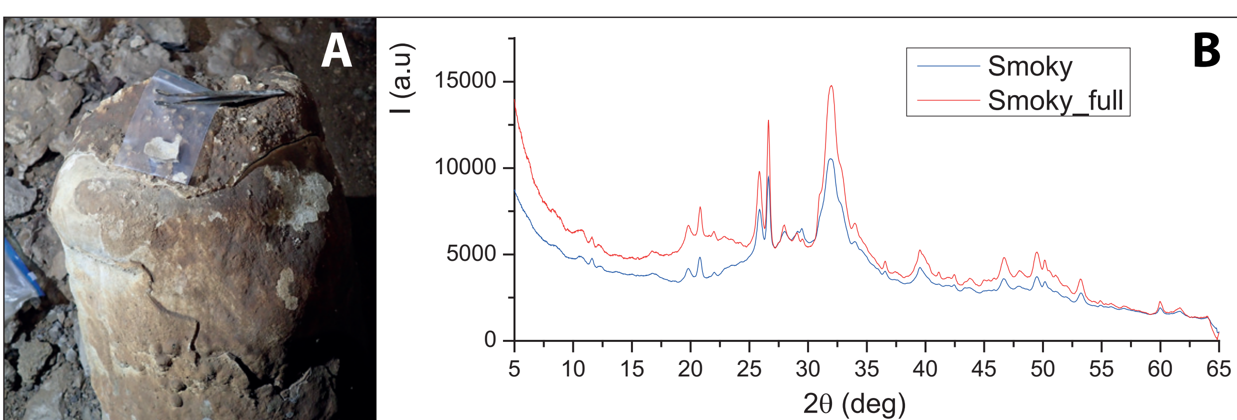

Fig. 13: A) Old corroded stalagmite, covered by a thin apatite crust, Smoky Cave (Photo: D. Cailhol). B) DRX pattern of the brown crust (analysis from Heresanu, CINaM lab).

Tab. 2: Climatic data measured in caves.

Name of cave	Temperature (°C)	Relative humidity (RH, in %)	CO_2 (ppm)	Location of measurement	Month/ Year
Smoky Cave	17.7 °C	88.6%	540	Bottom of entrance shaft	May 2018
	15.2 °C 15.3 °C	99.9%	600 689	Bottom Chamber	Dec. 2017 May 2018
Pigeons Cave	17.8 °C	80.0%		Bottom	May 2018
First Day Cave	20.2 °C	67%	443	End of East lateral passage: strong and cool airflow, entering cave, descending from plateau surface	May 2018
	32 °C	32%	440	Outside air	May 2018
Fig Tree Cave	17.7 °C	88.5%	530	Final Chamber, 2 m high	May 2018
	17.8 °C	93.5%	547	Final Chamber, floor	
	18.1 °C	99.5%	1000	Passage to Final Chamber, fissure in the ceiling	
	18.2 °C	95.5%	660	Passage to Final Chamber, ceiling channel	
	18.2 °C	96.4%	565	Passage to Final Chamber, 50 cm high	
	18.1 °C	96%	575	Passage to Final Chamber, floor	
	18.0 °C	82%	745	Feeder entrance, 50 cm high	
	18.3 °C	94.9%	605	Bottom of feeder	
	18.7 °C	99.9%	1000	Main passage 25 m to entrance, ceiling channel	
	18.1 °C	97%	620	Entrance, 2 m high	
	34 °C	22.5%	440	Outside air	

Tab. 3: DRX analysis results from samples of Smoky and Angry Bat caves (analysis CINaM).

Cave	Sample no.	Disp.	Identified phases	Observations
Smoky	Smoky	AT	Apatite, quartz, clay (illite) Probable gypsum Possible magnesian calcite, phillipsite	Surface of brown crust
Smoky	Smoky_full	AT	Same as Smoky	Brown crust, including its light lower part
Angry_Bat	Yellow powder	Xpert	Gypsum, calcite, quartz, clay (illite or muscovite)	More calcite than gypsum

*Tab. 4: 230Th dating results. The error is 2σ error. U decay constants: l_{238} = 1.55125x10^{-10} (Jaffey et al. 1971) and l_{234} = 2.82206x10^{-6} (Cheng et al. 2013). Th decay constant: l_{230} = 9.1705x10^{-6} (Cheng et al. 2013). * $\delta^{234}U = ([^{234}U/^{238}U]_{activity} - 1)x1000$. ** $\delta^{234}U_{initial}$ was calculated based on ^{230}Th age (T), i.e., $\delta^{234}U_{initial} = \delta^{234}U_{measured}\ x\ e^{l234xT}$. Corrected ^{230}Th ages assume the initial $^{230}Th/^{232}Th$ atomic ratio of 4.4 ±2.2 x10^{-6}. Those are the values for a material at secular equilibrium, with the bulk earth $^{232}Th/^{238}U$ value of 3.8. The errors are arbitrarily assumed to be 50%. ***B.P. stands for "Before Present" where the "Present" is defined as the year 1950 A.D.*

Sample Number	^{238}U (ppb)	^{232}Th (ppt)	^{230}Th / ^{232}Th (atomic x10^{-6})	$\delta^{234}U$* (measured)	^{230}Th / ^{238}U (activity)	^{230}Th Age (yr.) (uncorrected)	^{230}Th Age (yr.) (corrected)	$\delta^{234}U_{Initial}$** (corrected)	^{230}Th Age (yr. BP)*** (corrected)
SMOKY1-00	552.8 ±0.8	994 ±20	3,263 ±66	18.0 ±1.4	0,3560 ±0.0008	46,856 ±159	46,804 ±163	21 ±2	**46,736 ±163**
SMOKY2-01	336.0 ±0.5	797 ±16	2,438 ±49	12.9 ±1.5	0,3507 ±0.0008	46,301 ±155	46,233 ±162	15 ±2	**46,165 ±162**
Pentad00	109.0 ±0.1	167 ±4	10,485 ±224	181.6 ±1.2	0,9744 ±0.0014	174,720 ±751	174,685 ±751	297 ±2	**174,617 ±751**

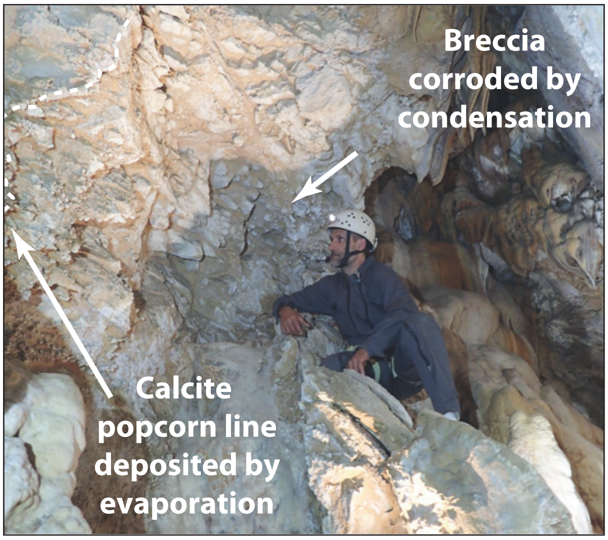

Fig. 14: Condensation-corrosion of breccia fault, with a calcite popcorn line at the edge, where evaporation occurs. In the background, brown-orange calcite flowstone, tinted by fresh guano. Above, a ceiling channel rises toward the top of the fracture (not visible). Smoky Cave (Photo: D. Cailhol).

Fig. 16: Recrystallized dolostone entirely weathered by dripping from condensation, strongly acidified by the nearby guano. Centimetric graduation on scale (Photo: D. Cailhol).

fied. In the first shaft, the ceiling had a half-cylindrical channel connected to the entrance that gradually disappeared inwards (Fig. 6). The surface of the ceiling channel was smooth, with no sign of calcite deposits. The curtains covering the overhanging wall appeared to be fed by runoff originating from this ceiling channel. However the host rock of this ceiling channel was extremely massive and did not present any evidence of seepage from the surface through fissures. In addition, at the end of the First Chamber, a 1.5 m wide channel rose along the overhanging wall toward the top of the fracture. Here, fresh guano was also present along the wall. In the same place, the wall locally consisted of fault breccia, where cement was deeply corroded but angular elements stood in relief. A calcite popcorn line delimited this deeply corroded zone (Fig. 14). No fluvial deposits and no marks of concentrated flow were present.

The active stalagmites of the wet Bottom Chamber displayed typical facies, made of thick layers of white lamina alternating with thinner layers of dark brown lamina (Fig. 15B). A discrete corrosive dripping had weathered and disaggregated a block of dolostone in the deepest part of the shaft (Fig. 16).

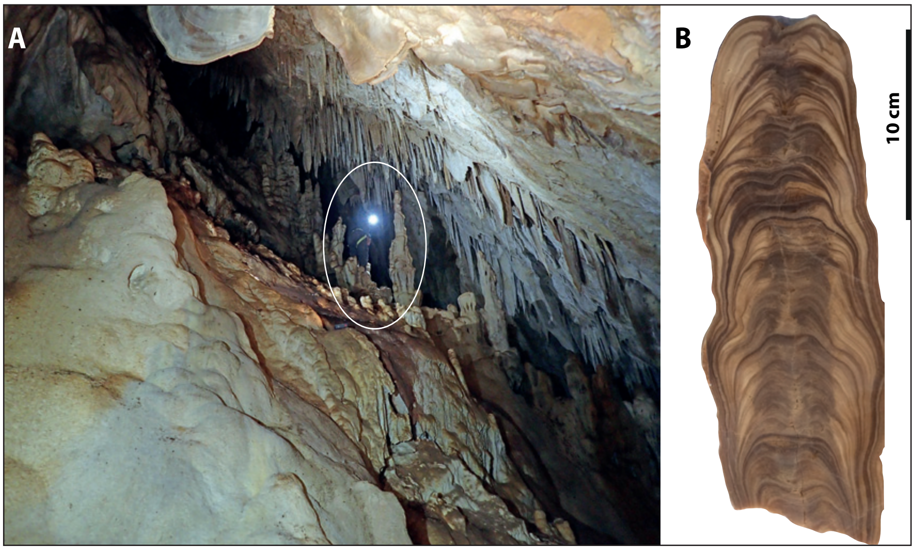

Fig. 15: A) Bottom chamber in Smoky Cave, developed along the opened inclined fracture. Note the abundance of flowstones that are affected nowadays by condensation moisture. Some flowstones are tinted in brown by fresh guano below cupolas harbouring bats roosting. Person for scale in the circle (Photo: D. Cailhol). B) Vertical section of a stalagmite. Thick layers of white lamina alternate with thinner layers of dark brown lamina. On a hypothetical basis, the dark brown colour could originate either from soil organic contamination or from guano byproducts, and in the latter case could record the periodical presence of bats (Photo: P. Audra).

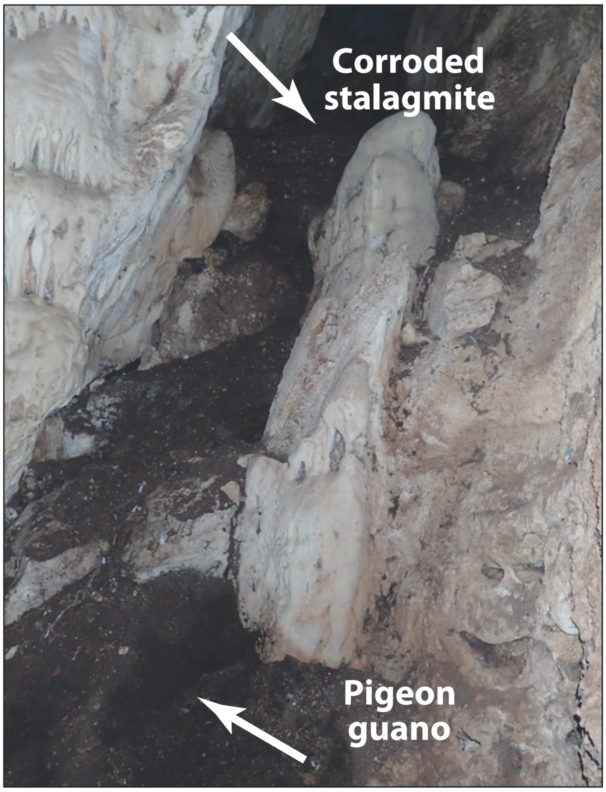

Fig. 17: Pigeons Cave, bottom of the fracture. Flowstone deeply corroded by condensation-corrosion, floor covered by pigeon guano. Width of the fracture ≈1.2 m (Photo: D. Cailhol).

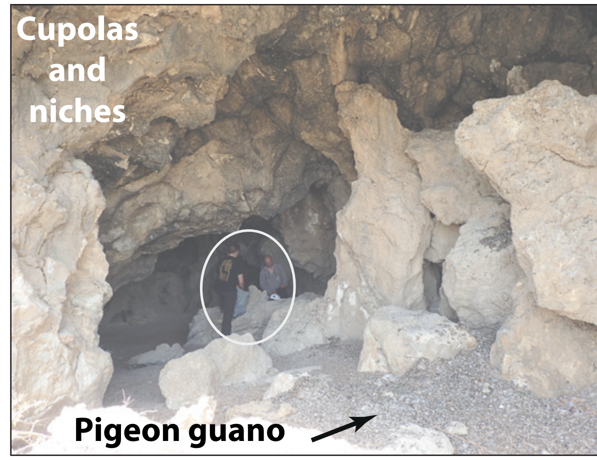

Fig. 18: Entrance of First Day Cave. In foreground, collapsed blocks covered by pigeon guano. Round morphologies (cupolas, niches) are carving the ceiling and the walls. Two persons for scale in the circle (Photo: D. Cailhol).

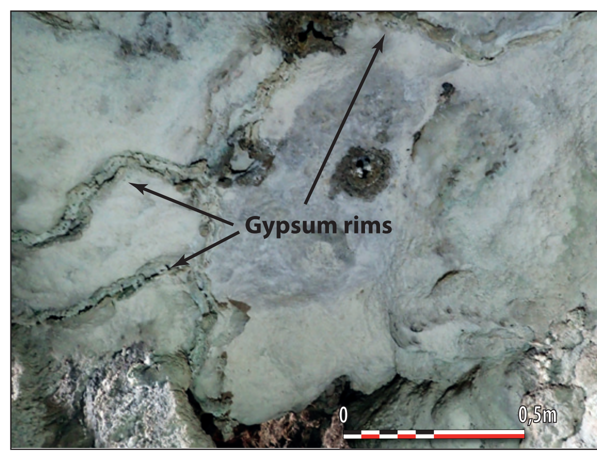

Fig. 19: First Day Cave. Gypsum rims made by evaporation of moisture provided par capillarity runoff outflowing from decompression fractures (Photo: D. Cailhol).

PIGEONS CAVE

The cave temperature was 17.8 °C (May 2018) and lower (-0.3 °C) than the local mean annual temperature (Tab. 2). The RH was 80.0% (May 2018) inside the cave, which was entirely dry. Some massive stalagmites and corroded flowstones were present at the bottom (Fig. 17). The floor was covered by a thick (0.5–1 m) layer of pigeon guano. No fluvial morphologies and related deposits were observed in this cave.

FIRST DAY CAVE

A strong and cool airflow (20.2 °C; 67% RH) was entering the cave from the end of the East lateral passage, descending from the plateau surface, in May 2018 (Tab. 2). Such important airflow is driven by the high temperature gradient. The main gallery and the West gallery displayed round morphologies (cupolas, round blind ends, arches, lateral niches) that covered all walls and ceilings (Fig. 18). The East fractures showed smoothed walls and ceiling channels similar to a vadose meander. In the entire cave, a constant vertical distribution of features was observed: the ceiling and the upper part were smooth and exposed with no crust features. However, in the lower part of the cave section, a gypsum crust with nodular morphology gradually appeared and thickened downwards with more than 10 cm thickness. In the West gallery, the ceiling cupolas intersected as round reliefs that collect the runoff from cupolas and produced small stalactites and their correspondence on the floor. Some open-fractures, parallel to the cliff, intercepted the cave walls of the main gallery and displayed some gypsum rims (Fig. 19). No fluvial morphologies and deposits were observed inside the cave.

ANGRY BAT CAVE

The ceiling was carved by a slightly rounded channel. Together with the upper part of the passage, the cave wall was exposed, smooth and showing corrosion processes. The lower part of the cave wall, however, was covered by gypsum crust, thickening downwards (Fig. 11). A thin (1 cm) layer of yellowish dry powdery crys-

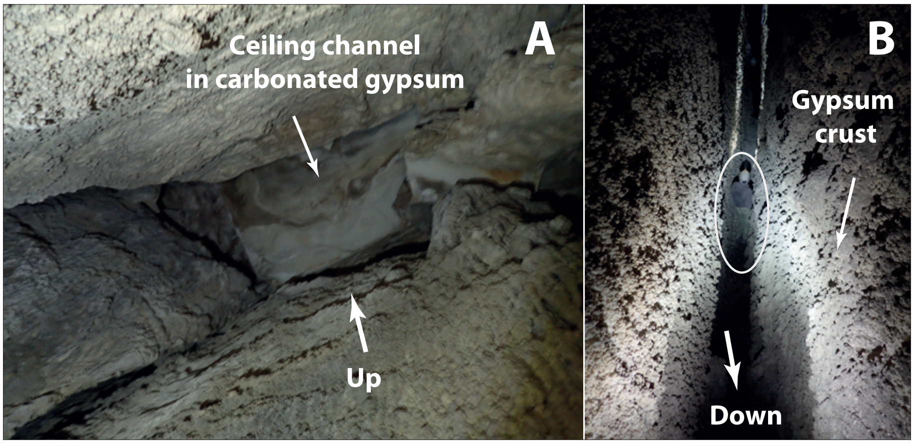

Fig. 20: Angry Bat Cave. A) View toward the ceiling, about 1 m in width (Photo: D. Cailhol). B) View along the inner fracture (person for scale in the circle). Ceiling and upper parts of the wall are exposed, smoothed by condensation-corrosion along the cooler ceiling, while lower part of the wall shows a gypsum crust thickening downwards by evaporation due to drier air at the bottom (Photo: D. Cailhol).

tals was inserted between the hard gypsum crust and the gypsum wall. DRX showed the presence of mainly calcite, then gypsum, with trace of detrital minerals (quartz and illite-muscovite). The wall surface displayed gypsum macrocrystals that were vertically cut with sharp edges showing a levelled corrosion below the crust. Bat guano covered the floor of the inner fracture passage. No fluvial morphologies or deposits were detected inside the cave.

FIG TREE CAVE

Passage profiles showed exposed and smooth channels on the ceiling and lateral notches with a flat roof at the entrance (Fig. 21). The notches developed at the same level, which also corresponded to the original level of the entrance (Fig. 12), before being partly constricted by collapsed blocks. Since the cave is located at the outlet of a valley crossing the gypsum plateau toward the Mesaoria Plain, the notches and the ceiling channels indicate an old outflow draining the gypsum aquifer.

A 5 m deep slot was visible at the end of the entrance gallery (Fig. 21C) with a patch of scallops at the bottom. It probably acted as a feeder during the phreatic stage, from which the water was rising from the depth to the main level. At the end of the cave, another slot probably acted in a similar way (Fig. 12). Moreover, in the end part, a passage was completely filled with fluvial sediments. They consisted of laminated yellowish-greenish silts, made up of 75% of carbonate and 25% of microcrystalline gypsum grains. The laminated cave deposits gradually fell apart in the gallery, exhuming the previously covered walls and showing sharp and levelled

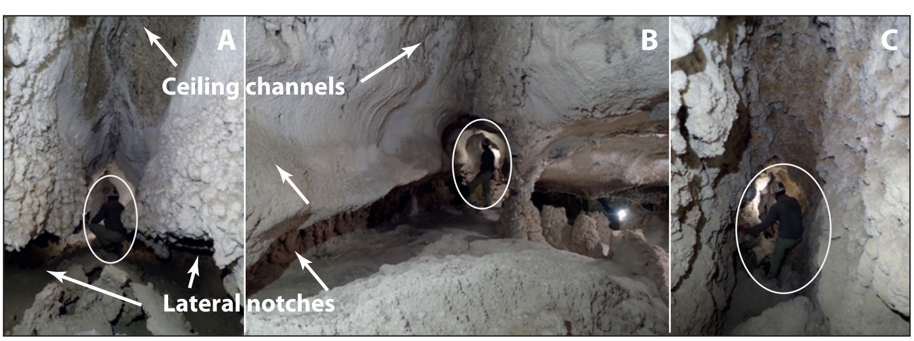

Fig. 21: Fig Tree Cave, phreatic features from the initial active phase. A-B) Ceiling channels from the early phreatic phase are located above lateral notches from a subsequent epiphreatic phase after partial dewatering (Photos: D. Cailhol). C) Downward view of the 5 m deep slot, probably a feeder from which water was flowing up (Photo: D. Cailhol).

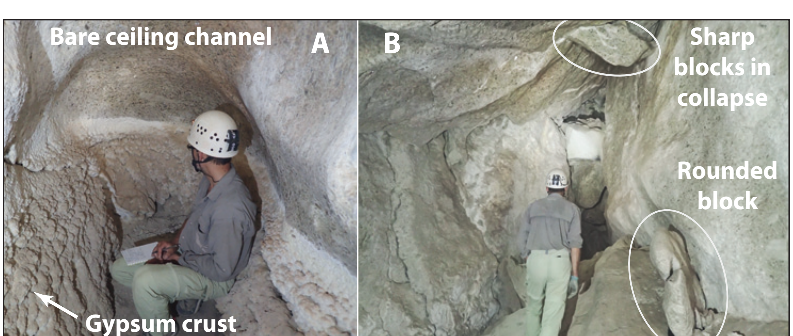

Fig. 22: Fig Tree Cave, condensation-corrosion features of the late phase. A) Round blind termination, with typical profile showing round ceiling channel with exposed rock where condensation-corrosion occurs on cooler ceiling, and lower walls covered by downwards thickening crusts of gypsum made by evaporation (Photo: D. Cailhol). B) Boulder choke in the final chamber, showing blocks with sharp edges in the collapse, whereas fallen blocks on the ground have been rounded and smoothed by condensation-corrosion (Photo: D. Cailhol).

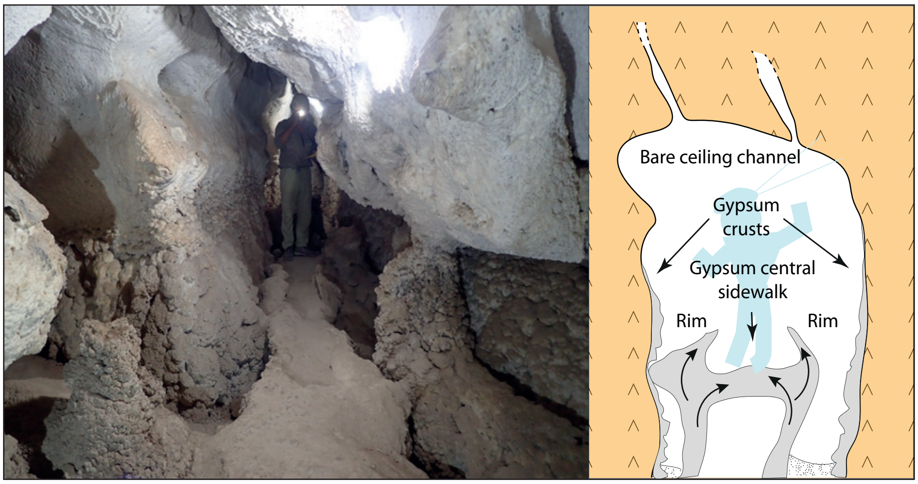

Fig. 23: Fig Tree Cave, evaporation features of the late phase. The upper part of the gallery with bare ceiling channel where condensation prevails is not visible in the picture. Lower walls are covered by a thick gypsum crust made up by evaporation of condensation runoff flowing from upper part. Central sidewalk built by joining rims growing upward from the ground by evaporation (Photo: D. Cailhol).

Tab. 5: ^{222}Rn concentrations measured in the slot at the end-part, Fig Tree Cave (M. Garašić).

^{222}Rn concentrations (Bq/m^3/s)	**Date**
29.387 29.560	16/03/2017
22.711	31/10/2017

gypsum crystals with a uniform corrosion at the contact of the deposit. These fine sediments also witnessed an old phreatic phase, transporting material from the aquifer itself.

Some passages end with rounded morphology (Fig. 22). Classical vertical distribution of features occurred, with exposed ceiling and upper walls, whereas the lower parts of the walls were covered by gypsum crust, thickening downwards (Fig. 22A) and decorated by abundant stalagmites. In the Final Chamber, a side passage was blocked by a collapse of angular blocks. The fallen blocks were rounded with no sharp edges (Fig. 22B). In the last passage leading to the end-part of the cave, two parallel rims joined to form a central sidewalk (Fig. 23). At the end of the entrance gallery, condensation runoff collected at the lower edge of the ceiling channel, creating a small stalactite that produced a drip hole in the gypsum ground.

The cave temperature (May 2018) ranged between 17.7 °C in the end-part of the cave and 18.7 °C along the ceiling at the entrance part. The RH inside the cave was around 80–90% at the cave floor and reached 95–100% along the cave ceiling (Tab. 2). It showed the possibility of condensation on the ceiling and evaporation on the floor.

A high concentration of SO_2 was detected near the cave floor (1 m above the floor). The CO_2 concentration was around 530 ppm along the cave floor and 1000 ppm along the ceiling. ^{222}Rn concentration, measured in the slot at the end-part (≈200 m from entrance; 13 m depth), displayed values between 22.000 and 30.000 Bq/m^3/s (Tab. 5).

DISCUSSION

We discuss the main results obtained regarding the morphological features of each cave as an expression of cave genesis, the relief evolution mainly resulting from tectonic history, the condensation-corrosion as a major late stage evolution process, and the effect of bat guano as a booster of the condensation-corrosion process.

MORPHOLOGICAL FEATURES AS AN EXPRESSION OF CAVE GENESIS

Smoky Cave

Since no initial fluvial stage occurred and since it is located on a crest with a negligible catchment above the cave, the rounded morphologies are obviously linked to condensation-corrosion. In warm periods, stable conditions with no significant airflow gradually lead to the equilibrium of the inner temperature. However, in cold periods, instability produces cold air inflow.

In the first shaft, convective airflow raises, cools, and canalizes along the ceiling toward the entrance, making condensation and eventually corroding the rounded ceiling channel (Fig. 6). Since the ceiling channel is carved into massive recrystallized carbonates, where few fissures are visible and seepage could only occurs during winter season, most of the water during late-spring and summer seasons is expected to come from condensation only (Frumkin *et al.* 2018). Therefore, the curtains along the overhanging wall would mainly be fed by moisture originating from the ceiling channel. The condensed water gradually saturates and evaporates while flowing (Bradley 2015). In the First Chamber, convection loops make local condensation-corrosion that carves the rising channel located at the end of the chamber and on the breccia zone. Due to the complex distribution of convective loops, this corroded breccia is surrounded by an evaporation zone delimited by a popcorn line (Frumkin *et al.* 2018). This results in evaporation of the moisture from the condensation zone (Fig. 14). Discrete drippings on guano deposits make colorful calcite flowstones. In the Bottom Chamber, the permanent moisture cannot be related to the epikarst seepage, especially in the dry season. This moisture would results from the presence of the bat colony releasing vapour, together with heat and CO_2, which are distributed by the local convection cells (Lundberg & McFarlane 2009, 2012, 2015; Frumkin *et al.* 2018). Moreover, the mineralization of guano releases acids (carbonic, nitric, phosphoric, and sulphuric) that strongly contribute to the aggressiveness of condensation water. Bat metabolism and guano mineralization are clearly responsible for the weathering of the blocks below the dripping points (Fig. 16), for the development of convection cupolas used as roost places, for the ceiling channels (Audra *et al.* 2018), and probably also for the active speleothems that are densely developed in this chamber (Fig. 15A).

Pigeons Cave

Similarly, it is located on a crest that excludes any initial fluvial stage, which is confirmed by the absence of characteristic morphologies and sediments. Consequently, the corrosion of the flowstone (Fig. 17) could only have occurred through condensation water, with its aggressiveness boosted by the mineralization of pigeon guano (Shahack-Gross *et al.* 2004). Since the cave is dry in the hot season, such condensation may prevail in the winter season, where cave air instability allows strong convections, with sinking of outer cold air and rising of the corresponding cooling warm air.

First Day Cave

It harbours a set of rounded features (cupolas, ceiling channels, niches) that cover the entire walls and ceilings (Fig. 18). Since no fluvial sediments or morphologies are present and since a past activity as outflow cave in unlikely, such rounded features clearly point toward a condensation-corrosion process. It occurs on the cooler ceiling and inside opened fractures, whereas evaporation and deposition of thick crusts occur close to the warmer and drier ground and at the rim of decompression fractures (Fig. 19; Gázquez *et al.* 2015). Such processes must mainly occur during winter, when cold air entering the main gallery along the floor returns outside while cooling along the ceiling. First Day Cave seems to be entirely enlarged by condensation-corrosion starting from opened-fractures. The option that this cave could be a relic of an old perched fluvial outlet cannot be ruled out, but it is unlikely since no evidence points toward such an origin. In the probable case of a condensation-corrosion enlargement, the resulting size of the passages (up to 4 m diameter) is significant.

Angry Bat Cave

For the same reasons, all smooth phreatic-like morphologies (slightly rounded channel, exposed upper walls) clearly result from condensation-corrosion processes and in turn from evaporation for the gypsum crust covering the lower walls. Here, the soft material sandwiched between the corroded wall and the gypsum crust, made of powdery crystals of calcite and gypsum could come either from the disaggregation of the more carbonated ceiling or from the crystallization of calcite by common-ion effect in sulphate-saturated solution, or from both. The presence of quartz and clay points toward at least a partial contribution of detrital component.

Fig Tree Cave

The cave clearly acted as a discharge point, as shown by lateral epiphreatic notches that are connected to the level of the entrance (Figs. 12 & 21). Ceiling channels, located 1–2 m above, could correspond to an early phreatic phase before the partial dewatering. The water had probably risen from the slot, acting as a feeder, as shown by the wall features that probably correspond to scallops. Additional feeders from the inner fractures are likely. These feeders drained the gypsum aquifer at a shallow depth, since the underlying flysch aquiclude is located only 10–15 m below the cave passages. The fine sediment filling the end-part is linked to this early active phase, probably related to the incision of the valley during the Late Pleistocene. However, the re-activation of an intra-messinian paleokarst, filled during the Pliocene transgression, cannot be ruled out (Mocochain *et al.* 2012). In a later phase, after a base-level lowering and water draining of the cave, airflow crosses the cave, making condensation-corrosion by cooling of warm air on the ceiling, and evaporation-deposition by warming of air flowing along the floor. Condensation-corrosion on the ceiling maintains an exposed and smooth rock surface, while evaporation along the floor favours the deposition of gypsum crusts (Fig. 22) and the upward development of rims that eventually join as a central sidewalk (Fig. 23).

MORPHO-TECTONIC EVOLUTION

The landscape evolution of the northern part of Cyprus is recent, consecutive to the emersion of the Kyrenia Range starting in the Early Pleistocene (Palamakumbura *et al.* 2016). Indeed, the Kyrenia Range emersion is subsequent to the uplift of the coastal mountain ranges in Lebanon and Syria that emerged earlier during the Oligocene (Nader 2011) and later during the Plio-Pleistocene. The karstification phase of the Kyrenia Range is therefore recent, resulting in the development of vertical fractures with no marked cave levels, whereas the karstification phases of the coastal Levantine Range resulted in several marked multi-level karst systems (Nehme *et al.* 2016).

As for the gypsum outcrops of the Mesaoria Plain, the evolution of the studied caves could have briefly occurred during the MSC (Mocochain *et al.* 2012), before its definitive emersion in the Pleistocene and therefore be considered older than the caves in Kyrenia Range.

Fracture-caves of the Kyrenia Range carbonates

Their origin obviously postdates the emersion of the Kyrenia Range in the Early Pleistocene. Caves in lower altitudes are obviously much more recent due to the later emersion. Caves at higher altitude could be of any age in this period, according to the successive tectonic phases. The U/Th dating applied on cave calcite give a minimal age to the cave evolution of Kyrenia. Three speleothems collected from Smoky and Pentadactylos caves (Tab. 4) showed ages at 46.7±0.16, 46.1±0.16, and 174.6±0.76 ka BP at their basal section, inducing a fracture opening phase prior to the end of the Middle Pleistocene period.

The fracture-caves are linked to the permanent activity of the transpressive faults that opened the N30°E conjugate pull-apart fractures. Eventually, they evolved by local collapses, probably in relation to seismic activity. Surprisingly, decompression fractures do not significantly affect caves, even near cliffs and steep slopes, which appear to remain relatively stable. Flowstones development occurred, especially during the wetter periods. Condensation-corrosion is at the origin of ceiling channels and the correlated evaporation-deposition produces popcorn lines (Smoky Cave). As a result, caves often display a geometric aspect with sharp walls and succession of shafts or chambers developed along the inclined faults, separated by constrictions due to rock fall accumulations. The floor consists of large collapsed blocks. Speleothems partly cover the walls and the floor. Only ceiling channels and some speleothems show intense but focused corrosion made by condensation from convective airflows, hence their similarity to phreatic morphologies, also carved by turbulent flow.

Caves in messinian gypsum

Two types of cave occur. The first type corresponds to caves located on top of the cliff, which originate from decompression fractures. Airflow at the origin of condensation-corrosion dramatically enlarged the initial narrow fractures, producing on top of walls and ceilings rounded features such as ceiling channels, cupolas, and wall niches. It eventually achieves wide phreatic-like morphologies (First day Cave), even though there had no initial fluvial phase. In the lower part of walls, evaporation makes thick gypsum crust. The second type corresponds to discharge caves (Fig Tree Cave). In the initial phreatic phase, water was rising from a shallow depth through feeders along fractures connected to a maze controlled by the fracture network, then converging to a main trunk. It eventually discharged at the current cave entrance acting as a spring in the valley. A moderate base-level lowering allows a partial dewatering of the cave and the development of epiphreatic wall notches. The late phase occurred after the draining of the cave when the valley became perched and abandoned. Airflow crossing the cave produced condensation-corrosion with exposed rock along ceiling channels. In the lower part of passages, warm and dry air allowing evaporation makes thick gypsum crusts and abundant gypsum stalagmites.

Finally, the microclimate of this cave shows very high concentrations of radon and sulphur dioxide. The detection of SO_2 is not frequent in caves. Apart from volcanic caves, very few cases are reported in the literature, such as in the caves of Acquasanta Terme, Italy (Galdenzi 2017) and in Cueva de Villa Luz, Mexico (Hose *et al.* 2000). In the last case, the high SO_2 concentration (>35 ppm), associated to high levels of CO_2 and H_2S, would have its origin in evaporites buried at depth in Tabasco oil fields and in the possibility of fast transfer to the surface along major fault lines. In Fig Tree Cave, the SO_2 gas could be related to the bacterial reduction of sulphates from the gypsum into sulphur, which in turn oxidizes in SO_2. The dry environment with the absence of water would possibly limit the oxidation into sulfuric acid, favouring SO_2 production by direct oxidation of the sulphur in the presence of air, as already observed by the authors (DC, PA) in Grotta Aqua Mintina, a very dry gypsum cave in Sicily, Italy. Another possibility would point toward a deep crustal origin associated to the proximity of major transpressive active faults. The ^{222}Rn concentrations measured in Fig Tree Cave were very high, about two orders of magnitude higher than the usual values measured in caves (Field 2007). Lower values were recorded at the end of the dry season, whereas higher values correspond to the rainy season and to a period of tectonic activity in the northeastern part of the island. Surprisingly, CO_2 concentration remains in the normal range. Accordingly, the high concentrations of sulphur dioxide and radon could possibly be related to deep-seated fluids originating from the neighbouring transpressive fault activity, or, for the SO_2 only, to sulphate redox in very dry conditions.

Because of high solution rates, gypsum karst is known for its fast changes. However, the semi-arid climate of Cyprus must slow down its evolution. Decompression caves are clearly connected to the current retreat of the cliff, which however appears to be moderate. The discharge Fig Tree Cave developed in relation to the evolution of the valley, which is now perched and abandoned. The age of the caves is still unknown, but their close connection to the recent landscape would suggest a Late Pleistocene age.

CONDENSATION-CORROSION AS MAJOR LATE STAGE PROCESS IN SEMI-ARID CLIMATE

In addition to the common processes of cave evolution, such as block collapse and speleothems deposition, condensation-corrosion acts as a major process in the late stage of cave evolution. Condensation-corrosion is at the origin of rounded and smooth features (ceiling channels, corroded speleothems, and focused zones of rock wall corrosion). Due to the similar behaviour of airflow fluid, such features resemble phreatic morphologies, making it difficult to identify their true origin in most of the caves. In the studied fracture-caves of Cyprus apart Fig Tree Cave, in both carbonate and gypsum, where no initial phreatic phase has occurred, these rounded features located only in the upper part of the passages must be assigned to condensation-corrosion only. Such characteristic of Cyprus fracture-caves is fundamental for studying the role of condensation-corrosion and its extent. In such a dry environment, condensation may also be at the origin of moisture. After the wall corrosion and gradual saturation, produced water flows along walls and produces calcite precipitation such as the curtains of Smoky Cave. Due to the apparent absence of dripping from epikarst seepage through the massive recrystallized carbonate rock, some of the speleothem's late evolution could be related to condensation-corrosion (Frumkin *et al.* 2018).

The correlative process of condensation-corrosion by cooling airflow occurring from convection cells is the evaporation of sinking cool air that warms along the cave bottom. In carbonate caves, evaporation favours the precipitation of calcite popcorns around wet zones. In gypsum caves, it is at the origin of massive gypsum stalagmites and thick gypsum crusts covering the lower part of walls. Sidewalk rims, made by the coalescence of upwardly growing rims, are uncommon features.

Condensation-corrosion activity follows a seasonal trend. In summer, descending caves with only one entrance have a stable atmosphere. Colder cave air is trapped and exchanges are limited to barometric changes and wind pulses that can push air in and out. On the contrary, in winter, the unstable cave atmosphere allows cold surface air to enter the caves, triggering powerful convections that blow out inner warm air. This latter condenses while cooling and produces a cloud outside the cave by mixing with cold atmospheric air, hence the name of Smoky Cave (Fig. 6). Cold inflowing air is gradually warmed at the contact of the rock, which is warmer, and probably by the presence of the bat colony that release heat and vapour. Such winter inflow of cold air also explains why its bottom temperature is more than 1 °C lower than the mean local temperature at this altitude, due to a dominant effect of surface temperature during winter, typical of such "cold traps". This is the case of many fracture-caves in carbonate rocks. Caves with two entrances located at different altitudes are almost permanently ventilated by the chimney effect, with ascending airflow in winter (cave air warmer than outside) and descending airflow in summer (cave air cooler than outside). Inner temperature is thus influenced at the proximity of the inflowing entrance: in May 2018, Fig Tree Cave temperature was 1.4 °C lower than the surface average, due to previous cooling by strong air flow entering during the previous winter (Fig. 12); on the contrary, First Day Cave, which is close to the engulfing entrance was already 0.8 °C warmer in May than the surface average. Pigeons Cave is a mixed case, acting as a cold trap in winter combined to ventilation with another entrance, providing a temperature of only 0.3 °C lower than the surface average. Such a dynamic is important, since rock wall cooling in winter increases the temperature gradient and thus condensation volume. On the contrary, in summer, hot (35–45 °C) and dry external air (RH < 30%) entering in fresh caves is not sufficient to reach the dew point, even by a cooling of up to 10–15 °C: caves remain dried by airflow. Such seasonal dynamic was previously noticed in Sorbas caves, South Spain, which has a climate similar to Cyprus, where condensation mainly occurs in winter (Gázquez *et al.* 2017). Isotope ratios have also shown that the solution at the origin of gypsum crusts and speleothems is made of 60% of condensation water and the rest of seepage water. Consequently, in Cyprus, the peak of condensation probably occurs in winter, in both gypsum and carbonate caves.

The volume of the corroded rock by condensation-corrosion is difficult to quantify. Long cave climatic data, including temperature, RH, and pCO_2, are missing and insufficient for such quantification. Extrapolation to any rock volume corrosion would assume a constant rate, which is obviously not the case. The morphological connection between the cave and the surface, allowing significant air exchange, is also a key point. However, for First Day cave, using the rates of wall retreat (3.3 cm/ka) calculated for Sorbas caves (Gázquez *et al.* 2015) that develop in a similar climate, an estimation of its development would require about 100–200 ka, assuming constant rates of wall retreat.

ROLE OF BAT COLONIES AND GUANO DEPOSITS

The presence of bat colonies is recognized as an important factor for increasing corrosion, especially when it occurs from condensation (Lundberg & McFarlane 2009, 2012, 2015; Frumkin *et al.* 2018; Audra *et al.* 2016 and reference therein). Bats contribute to cave climate change by their metabolism and their breath, providing significant amounts of heat, vapour, and CO_2. The mineralization of guano accumulations also provides heat, combined with acid production (carbonic, phosphoric, sulfuric, and nitric). Not only the floor is carved by guano acids, but also convection cupolas develop very fast by condensation boosted in such acidic environments, together with ceiling channels, wall retreat, corrosion of flowstones, *etc.* We assume that pigeon guano can have a comparable effect, but probably more limited, since grain-feeding animals provide less aggressive catabolic byproducts (Shahack-Gross *et al.* 2004).

Since no seepage from epikarst occurs in the dry season in Smoky Cave, the presence of a bat colony in the semi-confined Bottom Chamber could probably be at the origin of the permanent moisture. The activity of speleothems, which is permanent only in this area, could also be related to bat moisture. Similarly, alternating white and brown lamina have been observed in some speleothems from Smoky Cave. The origin of the brown color is still unknown. It could originate either from soil organic infiltration and precipitation or from guano byproducts and in that case could record the temporary presence of bats.

Finally, such bat-related acidic sources are not active in gypsum caves, since the solubility of this mineral is not significantly influenced by acidity. In gypsum caves, even if bats are present, only the condensation volume can explain the development of the observed corrosion features.

CONCLUSION

- Two types of caves were studied in Cyprus: firstly, fracture-caves in the Kyrenia Range carbonates as pull-apart open-voids derived from the transpressive fault activity, and as decompression fractures on top of gypsum cliffs; secondly one discharge cave in gypsum as fracture-guided mazes fed by deep feeders.
- Late stage of cave evolution was governed by condensation-corrosion, after opening to the surface with air exchanges and potentially colonization by bats (Fig. 24).
- The advantage of fracture-caves is that most of them had never undergone the usual initial phreatic flow, so that discrimination with phreatic morphologies, which is generally equivoque in other areas, is not questionable here. Condensation-corrosion is the only process able to carve rounded morphologies made by convective airflows. Consequently, rounded morphologies (ceiling channel, cupolas, wall niches, and corroded flowstones) are made by airflow convections driving condensation-corrosion processes (Fig. 24).
- The correlative evaporation produces popcorn lines in carbonate caves; in gypsum caves it produces thick gypsum crusts, massive gypsum stalagmites, and sidewalk rims, which are uncommon features.
- Since in summer inflowing air is too dry to provide significant moisture in such a semi-arid climate, it seems that most of the condensation occurs in winter, when the instability of the cave atmosphere allows renewing of the inner cave air in both "cold trap caves" and caves where air is flowing between two entrances.
- Some gypsum fracture-cave enlargement through condensation-corrosion could reach up to 4–5 m width, that would require about 100–200 ka, according to wall retreat rates obtained in Southern Spain.
- Bat colonies significantly increase the aggressiveness of condensation-corrosion in carbonate caves, providing permanent moisture, vapour, heat, CO_2, and guano that releases heat and acids. Pigeon guano possibly has a similar effect, although probably less efficient.
- Caves are recent, and developed with the uplift of the

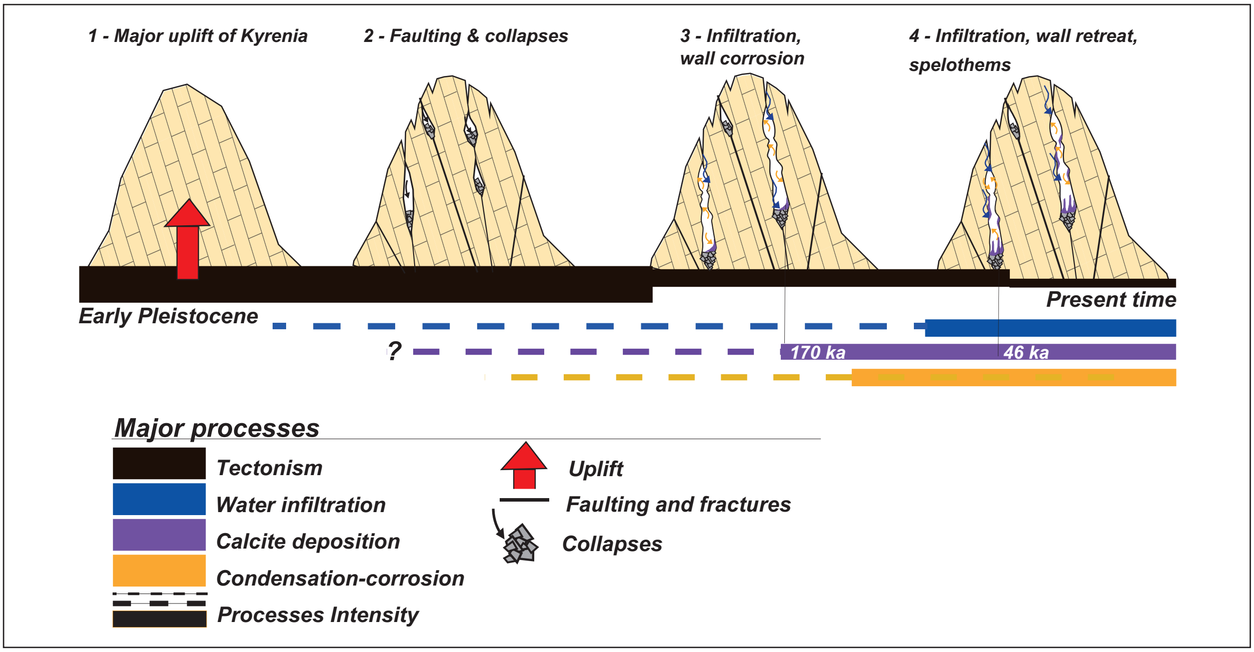

Fig. 24: Speleogenesis evolution of the Kyrenia Range. Fracture caves produced by faulting after fast uplift in Early Pleistocene. After opening to the surface, condensation-corrosion occurs. Calcite deposition record occurs since Middle Pleistocene.

Kyrenia Range during the Pleistocene, and especially during the Late Pleistocene for gypsum caves.

- High concentrations of SO_2 and ^{222}Rn detected in Fig Tree gypsum cave could be partly related to the activity of the neighbouring transpressive fault.

Although they seem inactive and dry, the studied Cypriot caves are still currently evolving under the condensation-corrosion process. Even with no flowing water and very limited dripping, the speleogenetic process is still fully active and produces ongoing corrosion morphologies and speleothems in caves that have a relict appearance.

Future research should integrate ongoing cave climate monitoring in Smoky and Fig Tree caves, to better assess and quantify air exchanges and condensation-corrosion processes. First U/Th dating of stalagmites in Smoky Cave provided a minimal age for the opening of fracture caves and a chronological frame for the development of the condensation-corrosion morphologies in this cave. High-resolution isotopic data would help to better figure out the part of seepage and condensation on speleothems building in such environment. Finally, measurements of SO_2 and radon concentrations, together with sulphur isotopes in Fig Tree Cave could confirm a deep-seated origin for gas released from the current activity of the nearby transpressive fault.

ACKNOWLEDGEMENTS

This study was conducted as part of the project '*The Caves of Kyrenia Mountains Project: Research, Conservation, and Education*' (Gucel 2018), supported by the European Union "Cypriot Civil Society in Action V" program (contract number: 2015/371- 989), the US Embassy in Nicosia, and the University of Rouen with the IRHIS funding for BQR-SHS 2018 grant. The research was led by Mağara Meraklıları Derneği ("Cave Enthusiasts NGO") in Nicosia, the University of Nicosia, and by the Union Internationale de Spéléologie (UIS; headquarter in Slovenia). We thank Mustafa Meraklı for abundant logistical support and for guiding us to the entrances of most caves studied here, the Spéléo-club du Liban (SCL) and the Croatian Speleological Federation (HSS) for cooperation on the field and for caves surveying. We also thank Ludovic Mocochain and Art Palmer for discussions during the preparation of this paper and Christian Dodelin for the identification of bat species. Finally, the thoughtful comments of reviewers greatly helped improve the manuscript.

REFERENCES

Audra, P., Barriquand, L., Bigot, J.-Y, Cailhol, D., Caillaud, H., Vanara, N., Nobécourt, J.-C., Madonia, G., Vattano, M. & M. Renda, 2016: L'impact méconnu des chauves-souris et du guano dans l'évolution morphologique tardive des cavernes (The little known impact of bats and bat guano in the late stages of cave morphogenesis).- Karstologia, 68, 1–20.

Auler, A.S. & P.L. Smart, 2004: Rates of condensation corrosion in speleothems of semi-arid northeastern Brazil.- Speleogenesis and Evolution of Karst Aquifers, 2, 2, pp. 2. [Online] Available from: http://www.speleogenesis.info/pdf/SG6/SG6_artId3270.pdf [accessed January 31st 2019].

Avramides, P.M., 2000: *Marble tombstones as environmental indicators*.- School of Chemistry, The University of Sydney, NSW, Australia.

Badino, G., 1995: *Fisica del clima sotterraneo*.- Memorie dell'Istituto italiano di Speleologia, pp. 136. Bologna.

Badino, G., 2010: Underground meteorology - "What's the weather underground?".- Acta Carsologica, 39, 427–448. DOI : 10.3986/ac.v39i3.74

Bradley R.S. 2015: *Paleoclimatology*.- Academic Press, pp. 696. DOI: 10.1016/C2009-0-18310-1

Cheng, H., Edwards, R.L., Shen, C.C., Polyak, V.J., Asmerom, Y., Woodhead, J., Hellstrom, J., Wang, Y., Kong, X., Spötl, C., Wang, X. & E.C. Alexander Jr., 2013: Improvements in 230 Th dating, 230 Th and 234 U half-life values, and U-Th isotopic measurements by muAlti-collector inductively coupled plasma mass spectrometry.- Earth and Planetary Science Letters, 371–372, 82–91. DOI: 10.1016/j.epsl.2013.04.006

Chirol, B., & T. Savoi, 2015: *Histoire Spéléologique de Chypre - Le Dessous d'Aphrodite / Cyprus caving history - Aphrodite's hidden charms*.- Comité Spéléologique Régional Rhône-Alpes, pp. 124, Lyon.

Chirol, B., Lips, B. & J. Lips, 2017: - Expédition spéléologique à Chypre, 5 au 16 novembre 2017.- [Online] Available from: https://blog.crei.ffspeleo.fr/?cat=11 [accessed January 31st 2019]

Cigna, A. & P. Forti, 1986: The speleogenetic role of air flow caused by convection.- International Journal of Speleology, 15, 41–52. DOI: 10.5038/1827-806X.15.1.3

Cleintuar, M.R., Knox, G.J. & P.J. Ealey, 1977: The geology of Cyprus and its place in the East-Mediterranean framework.- Geologie en Mijnbouw, 56, 66–82.

Constantinou, G., 1995: *Geological Map of Cyprus, 1/250.000*.- Geological Survey of Cyprus.

Department of Meteorology, 2018: The climate of Cyprus. [Online] Available from: http://www.moa.gov.cy/moa/MS/MS.nsf/DMLcyclimate_en/DMLcyclimate_en?OpenDocument [accessed January 31st 2019].

Dreybrodt, W., Gabrovšek, F. & M. Perne, 2005: Condensation corrosion: a theoretical approach.- Acta Carsologica, 34, 2, 317–348. DOI: 10.3986/ac.v34i2.262

Dublyansky, V.N. & Y.V. Dublyansky, 2000: The Problem of Condensation in Karst Studies.- Journal of Cave and Karst Studies, 60, 1, 3–17. [Online] Available from: https://caves.org/pub/journal/PDF/V60/V60N1-Dublyansky.pdf [accessed January 31st 2019].

Fabbri, S., Sauro, F., Santagata, T., Rossi, G. & J. De Waele, 2017: High-resolution 3-D mapping using terrestrial laser scanning as a tool for geomorphological and speleogenetical studies in caves: An example from the Lessini mountains (North Italy).- Geomorphology, 280, 16–29. DOI: 10.1016/j.geomorph.2016.12.001

Field, M.S., 2007: Risks to cavers and cave workers from exposures to low-level ionizing α radiation from ^{222}Rn decay in caves.- Journal of Cave and Karst Studies, 69, 1, 207–228. [Online] Available from: http://www.caves.org/pub/journal/PDF/v69/cave-69-01-207.pdf [accessed January 31st 2019].

Frumkin, A., Aharon, S., Davidovich, U., Langford, B., Negev, Y., Ullman, M., Vaks, A., Ya'aran, S. & B. Zissu, 2018: Old and recent processes in a warm and humid desert hypogene cave: 'A'rak Na'asane, Israel.- International Journal of Speleology, 47, 3, 307–321. DOI: 10.5038/1827-806X.47.3.2178

Galdenzi, S., 2017: The thermal hypogenic caves of Acquasanta Terme (Central Italy).- In: Klimchouk A., Palmer A.N., De Waele J., Auler A.S. & P. Audra (eds.) *Hypogene Karst Regions and Caves of the World*, Springer, 169–183. DOI: 10.1007/978-3-319-53348-3_10

Gázquez, F., Calaforra, J.M., Forti, P., De Waele, J. & L. Sanna, 2015: The role of condensation in the evolution of dissolutional forms in gypsum caves: Study case in the karst of Sorbas (SE Spain).- Geomorphology, 229, 100–111. DOI: 10.1016/j.geomorph.2014.07.006

Gázquez, F., Calaforra, J.M., Evans, N.P. & D.A. Hodell, 2017: Using stable isotopes ($\delta^{17}O$, $\delta^{18}O$ and δD) of gypsum hydration water to ascertain the role of water condensation in the formation of subaerial gypsum speleothems.- Chemical Geology, 452, 34–46. DOI: 10.1016/j.chemgeo.2017.01.021

Gucel, S., 2018: Caves of the Kyrenia Mountains: research, education, and conservation.- In: Prelovšek, M. (ed.): *Show caves and Science : abstracts & guide book, 26th International Karstological School "Classical Karst", Postojna, 2017.* ZRC Publishing, Postojna, 70–71.

Harrison, R., Newell, W., Panayides, I., Stone, B., Tsiolakis, E., Necdet, M., Batihanli, H., Ozhur, A., Lord, A., Berksoy, O., Zomeni, Z. & J.S. Schindler, 2008: *Bedrock geologic map of the greater Lefkosia area, Cyprus*.- U.S. Geological Survey Scientific Investigations, Map 3046, pp. 36. [Online] Available from: https://pubs.usgs.gov/sim/3046/pdf/pamphlet-sim3046.pdf [accessed January 31st 2019].

Harrison, R.W., Tsiolakis, E., Stone, B.D., Lord, A., McGeehin, J.P., Mahan, S.A. & P. Chirico, 2013: Late Pleistocene and Holocene uplift history of Cyprus: implications for active tectonics along the southern margin of the Anatolian microplate.- Geological Society, London, Special Publications, 372, 1, 561–584. DOI: 10.1144/SP372.3

Hose, L.D., Palmer, A.N., Palmer, M.V., Northup, D.E., Boston, P.J. & H.R. Duchene, 2000: Microbiology and geochemistry in a hydrogen-sulphide-rich karst environment.- Chemical Geology, 169, 399–423. DOI: 10.1016/S0009-2541(00)00217-5

Jaffey, A.H., Flynn, K.F., Glendenin, L.E., Bentley, W.C. & A.M. Essling, 1971: Precision measurement of half-lives and specific activities of ^{235}U and ^{238}U.- Physical Revue C, 4, 1889–1906. DOI: 10.1103/PhysRevC.4.1889

James, J.M., 2013: Atmospheric processes in caves.- In: Shroder, J. (Ed.) *Treatise on Geomorphology*. Academic Press, 304–318, San Diego. DOI: 10.1016/B978-0-12-374739-6.00118-4

Jameson, R.A., 1991: Features of condensation corrosion in caves of the Greenbrier karst, West Virginia.- National Speleological Society Bulletin, 53, 44. [Online] Available from: https://caves.org/pub/journal/NSS%20Bulletin/Vol%2053%20num%201.pdf [accessed January 31st 2019].

Jones W.F. & J. Rigby (Eds.) 1962: *Some Caves of Cyprus*.- Bristol Exploration Club Library, pp. 18, Bristol.

Jorgenson, B.T., 1978: Pentadaktylos Pot.- South Wales Caving Club Newsletter, 88, 12–13. [Online] Available from: http://www.swcc.org.uk/joomla-swcc/images/Documents/Docs_Arch/Newsletter/Newsletter88.pdf [accessed January 31st 2019].

Klimchouk, A., Cucchi, F., Calaforra, J.M., Aksem S., Finocchiaro, F. & P. Forti, 1996: Dissolution of Gypsum from field observations.- International Journal of Speleology, 25, 3–4, 37–48. DOI: 10.5038/1827-806X.25.3.3

Lismonde, B., 2002*: Climatologie du monde souterrain, tome 2, Aérologie des systèmes karstiques*.- Comité départemental de spéléologie de l'Isère, pp. 362, Grenoble. [Online] Available from: http://cds38.org/wp/wp-content/uploads/2013/04/climatologie_monde_souterrain-tome2.pdf [accessed January 31st 2019].

Lismonde, B., 2003: Limestone wall retreat in a ceiling cupola controlled by hydrothermal degassing with wall condensation (Szunyogh model).- Speleogenesis and Evolution of Karst Aquifers, 1, 2, 1–3. [Online] Available from: http://www.speleogenesis.info/directory/karstbase/pdf/seka_pdf4478.pdf [accessed January 31st 2019].

Lundberg, J. & D.A. McFarlane, 2009: Bats and bell holes: the microclimatic impact of bat roosting, using a case study from Runaway Bay Caves, Jamaica.- Geomorphology, 106, 1–2, 78–85. DOI: 10.1016/j.geomorph.2008.09.022

Lundberg, J. & D.A. McFarlane, 2012: Post-speleogenetic biogenic modification of Gomantong Caves, Sabah, Borneo.- Geomorphology, 157–158, 153–168. DOI: 10.1016/j.geomorph.2011.04.043

Lundberg, J. & D.A. McFarlane, 2015: Microclimate and niche constructionism in tropical bat caves: a case study from Mount Elgon, Kenya. -In: Feinberg J., Gao Y. & E.C. Alexander Jr. (eds.) *Caves and Karst Across Time*. Geological Society of America Special Paper, 516, pp. 19. DOI: 10.1130/2015.2516(17)

McCay, G.A. & A.H.F. Robertson, 2013: Upper Miocene–Pleistocene deformation of the Girne (Kyrenia) Range and Dar Dere (Ovgos) lineaments, northern Cyprus: role in collision and tectonic escape in the easternmost Mediterranean region.- Geological Society, London, Special Publications, 372, 1, 421–445. DOI: 10.1144/SP372.6

Miller, T., 2014. Bellholes: ceiling cavities eroded by bats in caves of the neotropical climates.- AGU Fall Meeting. [Online] Abstract available from: http://adsabs.harvard.edu/abs/2014AGUFMEP31C3581M [accessed January 31st 2019].

Mocochain, L., Clauzon, G., Robinet, J., Blanpied, C., Suc, J.-P., Gorini, C., Al-Abdala A. & F. Azki 2012: Messinian Erosional Surface in the Levantine margin: geodynamic implications. [Online] Abstract available from: https://www.researchgate.net/publication/258625371_Messinian_Erosional_Surface_in_the_Levantin_margins_geodynamic_implications [accessed January 31st 2019].

Nader, F.H., 2011: The petroleum prospectivity of Lebanon: an overview.- Journal of Petroleum Geology, 34, 2, 135–156. DOI: 10.1111/j.1747-5457.2011.00498.x

Necdet, M., 2003: Overview of the karst occurrences in Northern Cyprus.- Acta Carsologica, 32, 2, 269–276. DOI: 10.3986/ac.v32i2.354

Nehme, C., Jaillet, S., Voisin, C., Hellstrom, C., Gérard-Adjizian, J. & J.J. Delannoy, 2016: Control of cave levels in Kanaan, Kassarat and Jeita karst systems (Central Mount Lebanon, Lebanon).- Zeitschrift für Geomorphologie, 60, 2, 95–117. DOI: 10.1127/zfg/2016/0239

Palamakumbura, R. & A.H.F. Robertson, 2016: Pliocene–Pleistocene sedimentary–tectonic development of the Mesaoria (Mesarya) Basin in an incipient, diachronous collisional setting: facies evidence from the north of Cyprus.- Geological Magazine, 1–26. DOI: 10.1017/S0016756816001072

Palamakumbura, R.N., Robertson, A.H.F., Kinnaird, T.C., van Calsteren, P., Kroon, D. & J.A. Tait, 2016: Quantitative dating of Pleistocene deposits of the Kyrenia Range, northern Cyprus: implications for timing, rates of uplift and driving mechanisms.- Journal of the Geological Society, 173, 6, 933–948. DOI: 10.1144/jgs2015-130

Sanna, L., De Waele, J., Calaforra, J.M. & P. Forti, 2015: Long-term erosion rate measurements in gypsum caves of Sorbas (SE Spain) by the Micro-Erosion Meter method.- Geomorphology, 228, 213–225. DOI: 10.1016/j.geomorph.2014.09.009

Satterfield, L., 2015: Launching the Caves of Cyprus Project.- NSS News, 4, 10–13.

Shahack-Gross, R., Berna, F., Karkanas, P. & S. Weiner, 2004: Bat guano and preservation of archeological remains in cave sites.- Journal of Archaeological Science, 31, 1259–1272. DOI: https://doi.org/10.1016/j.jas.2004.02.004

Spéléo-club du Liban, 2018: Reports and maps of caves (unpublished).

Tarhule-Lips, R.F.A. & D.C. Ford, 1998a: Condensation corrosion in caves of Cayman Brac and Isla de Mona.- Journal of Cave and Karst Studies, 60, 84–95. [Online] Abstract available from: http://w.caves.org/pub/journal/PDF/V60/V60N2-Tarhule-Lips.pdf [accessed January 31st 2019].

Tarhule-Lips, R.F.A. & D.C. Ford, 1998b: Morphometric studies of bell hole development on Cayman Brac.- Cave and Karst Science, 25, 119–130. [Online] Abstract available from: http://cavescience2-cloud.bcra.org.uk/3_CaveAndKarstScience/cks075.pdf [accessed January 31st 2019].

Unit of Environmental Studies, 2018: *The Pentadaktylos Zone.*- Cyprus geological heritage educational tool, Research and Development Center Intercollege. [Online] Available from: http://www.cyprusgeology.org/english/2_5_geology.htm [accessed January 31st 2019].